

AD-A150 512

ROBUST FEEDFORWARD/FEEDBACK CONTROL LOGIC FOR A
TARGET-TRACKING MECHANICA. (U) STANFORD UNIV CA DEPT OF
AERONAUTICS AND ASTRONAUTICS R H CANNON ET AL.

1/1

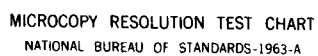
UNCLASSIFIED

08 MAR 84 SUDAR-537 AFOSR-TR-84-1277

F/G 6/4

NL

END



MICROCOPY RESOLUTION TEST CHART
NATIONAL BUREAU OF STANDARDS-1963-A

AD-A150 512



(12)

**ROBUST FEEDFORWARD/FEEDBACK CONTROL
LOGIC FOR A TARGET-TRACKING
MECHANICAL ARM**

Professor Robert H. Cannon, Jr., Chairman

Bruce E. Gardner, Research Assistant

Guidance and Control Laboratory
Department of Aeronautics and Astronautics
STANFORD UNIVERSITY
Stanford, California 94305

This research was supported by
The United States Air Force
USAF No. F49620-82-C-0092

THIS COPY

Approved for release
distribution unlimited

March 8, 1984

85 02 06 014

**ROBUST FEEDFORWARD/FEEDBACK CONTROL LOGIC
FOR A TARGET-TRACKING MECHANICAL ARM**

by

Professor Robert H. Cannon, Jr., Chairman

Bruce E. Gardner, Research Assistant

**Guidance and Control Laboratory
Department of Aeronautics and Astronautics
STANFORD UNIVERSITY
Stanford, California 94305**

**This research was supported by
The United States Air Force
USAF No. F49620-82-C-0092**

March 8, 1984

Handwritten notes and a stamp are visible in the bottom right corner. The stamp includes the text "Dist" and "A-1".



UNCLASSIFIED

SECURITY CLASSIFICATION OF THIS PAGE

REPORT DOCUMENTATION PAGE

1a. REPORT SECURITY CLASSIFICATION		1b. RESTRICTIVE MARKINGS	
2a. SECURITY CLASSIFICATION AUTHORITY Unclassified		3. DISTRIBUTION/AVAILABILITY OF REPORT Approved for public release Distribution unlimited.	
2b. DECLASSIFICATION/DOWNGRADING SCHEDULE		4. PERFORMING ORGANIZATION REPORT NUMBER(S)	
5. MONITORING ORGANIZATION REPORT NUMBER(S) AFOSR-TR- 84 - 1277		6a. NAME OF PERFORMING ORGANIZATION Stanford University	
6b. OFFICE SYMBOL (If applicable)		7a. NAME OF MONITORING ORGANIZATION AFOSR	
6c. ADDRESS (City, State and ZIP Code) Guidance & Control Lab Dept of Aeronautics & Astronautics Stanford University, Stanford, CA 94305		7b. ADDRESS (City, State and ZIP Code) Bldg 410 Bolling AFB DC 20332-6448	
8a. NAME OF FUNDING/SPONSORING ORGANIZATION AFOSR		8b. OFFICE SYMBOL (If applicable) NE	
9. PROCUREMENT INSTRUMENT IDENTIFICATION NUMBER F49620-82-C-0092		10. SOURCE OF FUNDING NOS.	
10a. PROGRAM ELEMENT NO. 61102F		10b. PROJECT NO. 2306	
10c. TASK NO. A3		10d. WORK UNIT NO.	
11. TITLE (Include Security Classification) ROBUST FEEDFORWARD/ FEEDBACK CONTROL LOGIC FOR A TARGET-TRACKING MECHANICAL ARM			
12. PERSONAL AUTHOR(S) Professor Robert H. Cannon, Jr., Bruce E. Gardner			
13a. TYPE OF REPORT Sem.-Annual		13b. TIME COVERED FROM 30 SEP 83 TO 30 MAR 84	
14. DATE OF REPORT (Yr., Mo., Day) March 8, 1984		15. PAGE COUNT 64	
16. SUPPLEMENTARY NOTATION			
17. COSATI CODES		18. SUBJECT TERMS (Continue on reverse if necessary and identify by block number)	
FIELD		GROUP	
SUB. GR.			
19. ABSTRACT (Continue on reverse if necessary and identify by block number) <p>An analytic design study is conducted to demonstrate circumstances under which the inclusion of feedforward compensation in a target-tracking control scheme can be expected to offer significant performance gain (e.g. enough to justify cost of implementation). In particular, a target-tracking controller design problem for a mechanical arm is developed to assess quantitatively the capacity of feedforward to provide a quicker, more accurate tracking response over wide ranges of uncertainty or variability in the dynamic parameters of both plant and target.</p> <p>The Stanford Aeronautics and Astronautics Department Robotics Lab two-link, two-actuator mechanical arm, inherently a system with variable kinematic and dynamic parameters, provides an appropriate framework for this study. Using recent developments in the theory of quadratic synthesis of robust, low-order "optimal" controllers, control logic is developed both with and without feedforward - that enables the arm end point to track a physical target characterized in part by periodic motion of variable or uncertain frequency and phase.</p>			
20. DISTRIBUTION/AVAILABILITY OF ABSTRACT UNCLASSIFIED/UNLIMITED <input checked="" type="checkbox"/> SAME AS RPT. <input checked="" type="checkbox"/> DTIC USERS <input type="checkbox"/>		21. ABSTRACT SECURITY CLASSIFICATION UNCLASSIFIED	
22a. NAME OF RESPONSIBLE INDIVIDUAL JOSEPH W HAGER, Maj, USAF		22b. TELEPHONE NUMBER (202) 767-4933	
22c. OFFICE SYMBOL NE			

It is shown that, using relatively noise-free measurements of target position coordinates only, feedforward compensation can be expected to provide substantial reductions in tracking errors for given constraints on control effort, particularly when the range of variation in target frequency is large. As noise levels in the position measurements increase, the relative improvement in tracking accuracy (for a given level of control effort) offered by feedforward decreases. However, if target rate coordinates are also measured and used in the feedforward control scheme, the improvement is shown to be considerable even for fairly high noise levels in all target measurements.

Experimental verification of the predicted results contained herein is scheduled for the near future.

UNCLASSIFIED

ABSTRACT

✓ An analytic design study is conducted to demonstrate circumstances under which the inclusion of feedforward compensation in a target-tracking control scheme can be expected to offer significant performance gain, (e.g. enough to justify cost of implementation). In particular, a target-tracking controller design problem for a mechanical arm is developed to assess quantitatively the capacity of feedforward to provide a quicker, more accurate tracking response over wide ranges of uncertainty or variability in the dynamic parameters of both plant and target.

The Stanford Aeronautics and Astronautics Department Robotics Lab two-link, two-actuator mechanical arm, inherently a system with variable kinematic and dynamic parameters, provides an appropriate framework for this study. Using recent developments in the theory of quadratic synthesis of robust, low-order ^{optimal} controllers, control logic is developed - both with and without feedforward - that enables the arm end point to track a physical target characterized in part by periodic motion of variable or uncertain frequency and phase.

It is shown that, using relatively noise-free measurements of target position coordinates only, feedforward compensation can be expected to provide substantial reductions in tracking errors for given constraints on control effort, particularly when the range of variation in target frequency is large. As noise levels in the position measurements increase, the relative improvement in tracking accuracy (for a given level of control effort) offered by feedforward decreases. However, if target rate coordinates are also measured and used in the feedforward control scheme, the improvement is shown to be considerable even for fairly high noise levels in all target measurements. *By, it also includes: Transfer Mathematical Models.*

Experimental verification of the predicted results contained herein is scheduled for the near future.

AIR FORCE OFFICE OF TECHNICAL INFORMATION
NOTICE OF TRANSMISSION
This technical report is approved for public distribution is unlimited.
MATTHEW J. KEMPER
Chief, Technical Information Division

TABLE OF CONTENTS

<u>Section</u>	<u>Page</u>
Abstract	i
Table of Contents	ii
List of Figures	iv
List of Tables	vi
1.0 Introduction	1
2.0 Problem Layout and Design Approach	3
2.1 Choice of Controller Structure	6
2.2 Choice of Performance Criteria	13
2.3 Brief Description of "SANDY1" Design algorithm	14
3.0 Single-Link, Single-Actuator Model	20
3.1 Problem formulation	20
3.2 Compensator Descriptions	22
3.3 Controller Design and Performance Criteria	25
4.0 Design Results for 1L/1A Model	28
4.1 Nominal Parameter Case (NoFF vs. FSFF)	28
4.2 Effect of Arm Tip Mass Variations (NoFF vs. ESFF at $\omega_T = \omega_{T_{no.}}$)	32
4.3 Effect of Target Frequency Variations (NoFF vs. FSFF at $M_{tip} = M_{tip_{nom}}$)	34
4.4 Effect of Noise in Feedforward Measurement(s) (NoFF vs. ESFF at $a_{\omega_T} = a_m = 1.5$)	34

5.0 Two-Link, Two-Actuator Model	42
5.1 Problem formulation	42
5.2 Compensator Descriptions	44
5.3 Controller Design and Performance Criteria for 2L/2A Arm	47
6.0 Design Results for 2L/2A Model ($a_{\omega_T} = a_m = 1.5$, $\nu_{ff} = 5\%$)	50
7.0 Conclusions	62
8.0 References	64

LIST OF FIGURES

<u>Figure</u>	<u>Page</u>
1 Target Tracking Control Scheme with Feedforward Compensation	2
2 Target Tracking Application for 2L/2A Arms: Pick-up from Paint Spray Booth .	5
3 Controller Structure (I): "NoFF" (No Feedforward)	9
4 Controller Structure (II): "FSFF" (Full State Feedforward)	10
5 Near Equivalent to FSFF Controller of Fig. 4	11
6 Controller Structure (III): "ESFF" (Estimated State Feedforward)	12
7 Illustration of SANDY1 Definitions for Transient and Steady-State Criteria . .	19
8 Position Error Time Histories: NoFF vs. FSFF Nominal Parameters Case . . .	30
9 Control Torque Time Histories: NoFF vs. FSFF Nominal Parameters Case . . .	31
10 Effect of Arm tip Mass Variability on Transient Tracking: NoFF vs. FSFF	33
11 Effect of Target Frequency Variability on Transient Tracking: NoFF vs. FSFF	37
12 Effect of Target Frequency Variability on Steady-State Tracking: NoFF vs. FSFF	38
13 Effect of Noise in Feedforward Measurements on Transient Tracking: NoFF vs. FF1, FF2	39
14 Effect of Noise in Feedforward Measurements on Steady-State Tracking: NoFF vs. FF1, FF2	40
15 Robustness of Tracking Transient Response to Actual Variations in Target Frequency	55
16 Robustness of Steady State Tracking Response to Actual Variations in Target Frequency	56
17 Position Error Magnitude Histories of Tracking Controllers Nominal Parameters Case	58

18	Control Torque Histories of Tracking Controllers Nominal Parameters Case . .	59
19	Position Error Magnitude Histories of Tracking Controllers Worst Parameters Case	60
20	Control Torque Histories of Tracking Controllers Worst Parameters Case	61

LIST OF TABLES

<u>Table</u>	<u>Page</u>
1 Closed Loop Data for Optimized 1L/1A Controllers Designed for Nominal Parameter Case	29
2 Closed Loop Data for Optimized 1L/1A Controllers Designed for Five Parameter Conditions and $\nu_{ff} = 5\%$	41
3 Closed Loop Parameters for Optimized 2L/2A Controllers Designed for Five Parameter Conditions and $\nu_{ff} = 5\%$	53
4 Average Performance Data for Optimized 2L/2A Controllers Designed for Five Parameter Conditions and $\nu_{ff} = 5\%$	54
5 Comparative Controller Performance at Worst Case Initial Conditions versus Design Goals	57

1.0 INTRODUCTION

Feedforward compensation has been applied to specific control system tasks for some time. For target-tracking applications, feedforward will typically appear together with some appropriate combination of output error feedback compensation (including integral control) and plant inner loop (e.g. rate) feedback in the overall control scheme (see Fig. 1). One advantage of feedforward control is to quicken the plant tracking response by providing the controller with "early information" about the future target trajectory, thus reducing the transient portion of the tracking error. Another effect of feedforward can be realized in situations when an oscillating target is to be tracked and where the variability/uncertainty (v/u) associated with the target dynamic parameters (e.g. frequency of target oscillatory motion) is significant. For these cases, it is straightforward to show that integral control does not ensure zero steady-state error over the entire target parameter v/u range so that the feedforward controller parameter choices will have a significant impact on the steady-state errors in addition to the transient errors.

A drawback of feedforward control is that direct measurements of one or more target motion states must be obtained using additional sensors and noise filters, resulting in a more costly and complex control system to implement. The question is thus raised whether a single set of feedforward controller parameters can be determined that offers enough average performance improvement over the plant and target parameter v/u ranges to justify "costs". That is, can a feedback-only control scheme using error and plant rate measurements only be designed that affords nearly as good performance for lower cost and simpler implementation?

In this report, a target-tracking design problem is developed for a two-link, two-actuator mechanical arm to explore conditions under which feedforward can be expected to provide significant improvements over a simple feedback-only control scheme in both transient and steady-state tracking performance.

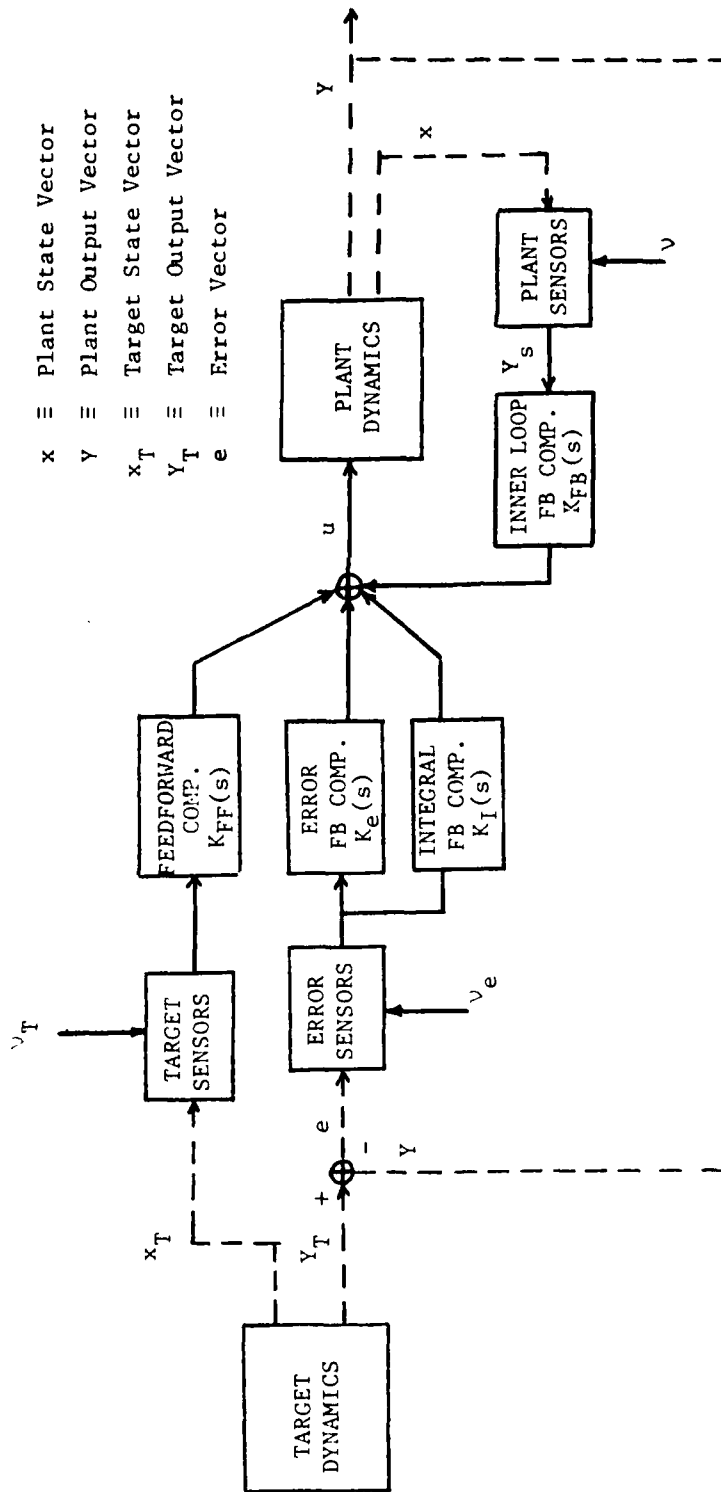


FIG. 1 TARGET TRACKING CONTROL SCHEME WITH FEEDFORWARD COMPENSATION
Inclusion of Feedforward Compensation is anticipated to provide a quicker, more accurate tracking response than error feedback compensation only

2.0 PROBLEM LAYOUT AND DESIGN APPROACH

The Stanford University Aero/Astro Robotics Laboratory two-link, two actuator (2L/2A) mechanical arm is nearing completion of construction.

One of the future tasks envisioned for this arm is to demonstrate ability to operate effectively in a target-tracking mode despite variability/uncertainty (v/u) in the arm and target dynamic parameters. Figure 2 is a schematic of a possible future target-tracking application for the 2L/2A arm. Here it is desired for the arm tip to track motions in the horizontal plane of an object suspended by a cable from an overhead conveyor belt moving at constant velocity v_{R_0} . The object is assumed to have recently passed through a paint-spray booth and, upon exit, continues to undergo natural, undamped oscillatory motion superimposed upon the rectilinear belt motion $y_R(t)$ at constant velocity v_{R_0} . Assuming a small nominal angle θ_0 between the attachment cable of length ℓ and the vertical reference, it can be shown [1] that, under ideal conditions, the linearized horizontal plane trajectory for the target object is approximated by a slowly precessing ellipse. The target completes one traversal of the ellipse every τ seconds, where

$$\tau_r = \frac{2\pi}{\omega_r} \quad \omega_r \approx \sqrt{\frac{g}{\ell}} \left(1 - \frac{\theta_0^2}{8}\right)$$

The precessional frequency of the major axis of the ellipse is given by:

$$\omega_{r_p} \approx \frac{3}{8} \theta_0^2 \sqrt{\frac{g}{\ell}}$$

In this work, it is assumed that θ_0 is small enough to neglect the precessional motion component. However, randomness associated with the ellipse amplitude, eccentricity, and orientation is accounted for as discussed in Section 3.1.

At time $t = 0^+$, the target-tracking control sequence is initiated. The goal is to cause the arm tip to track the target object to within a tolerance of ± 1 cm for all times greater than $t_s = 10$ seconds. In meeting (or exceeding) these error requirements, the torque

motor peak (rms continuous) limits of ± 15 N-m (± 3 N-m) are not to be violated.

At any time between t_0 and $t_f = 20$ secs (corresponding to the point $y_R(t_f)$ at which point the conveyor belt "ends"), a gripping mechanism of mass M_{tip} attached to the arm tip will thus be in reasonably good position to "reach up" and grasp the target object with low relative impact velocity and subsequently transfer the object to some other designated point in the assembly area. This control sequence (t_0, t_f) is to be continuously repeated throughout the daily operational hours of the assembly line.

Variable dynamic parameters associated with this problem are:

- (1) arm gripper mass (M_{tip})
- (2) target frequency of oscillation (ω_T)

The variations in M_{tip} and ω_T are taken to be discrete (e.g. due to sudden changes in gripper size and/or cable length by the plant operator to accomodate target objects of differing dimensions). However, it is assumed that all discrete changes in these parameters occur between tracking control sequences so that M_{tip} and ω_T are constant (although possibly unknown) during any single sequence (t_0, t_f) .

The designer's task is to devise an effective target-tracking control strategy which is in some sense "robust" to the v/u dynamic parameters. One approach to the problem would certainly be to consider the use of some type of adaptive control, such as gain scheduling in tandem with a parameter identification scheme for determining M_{tip} and ω_T . An alternative (and probably simpler to implement) approach is to design control logic using a single set of constant controller parameter values which, on the average, provides good tracking performance over the target and plant parameter v/u ranges. The latter approach is the one taken in this work.

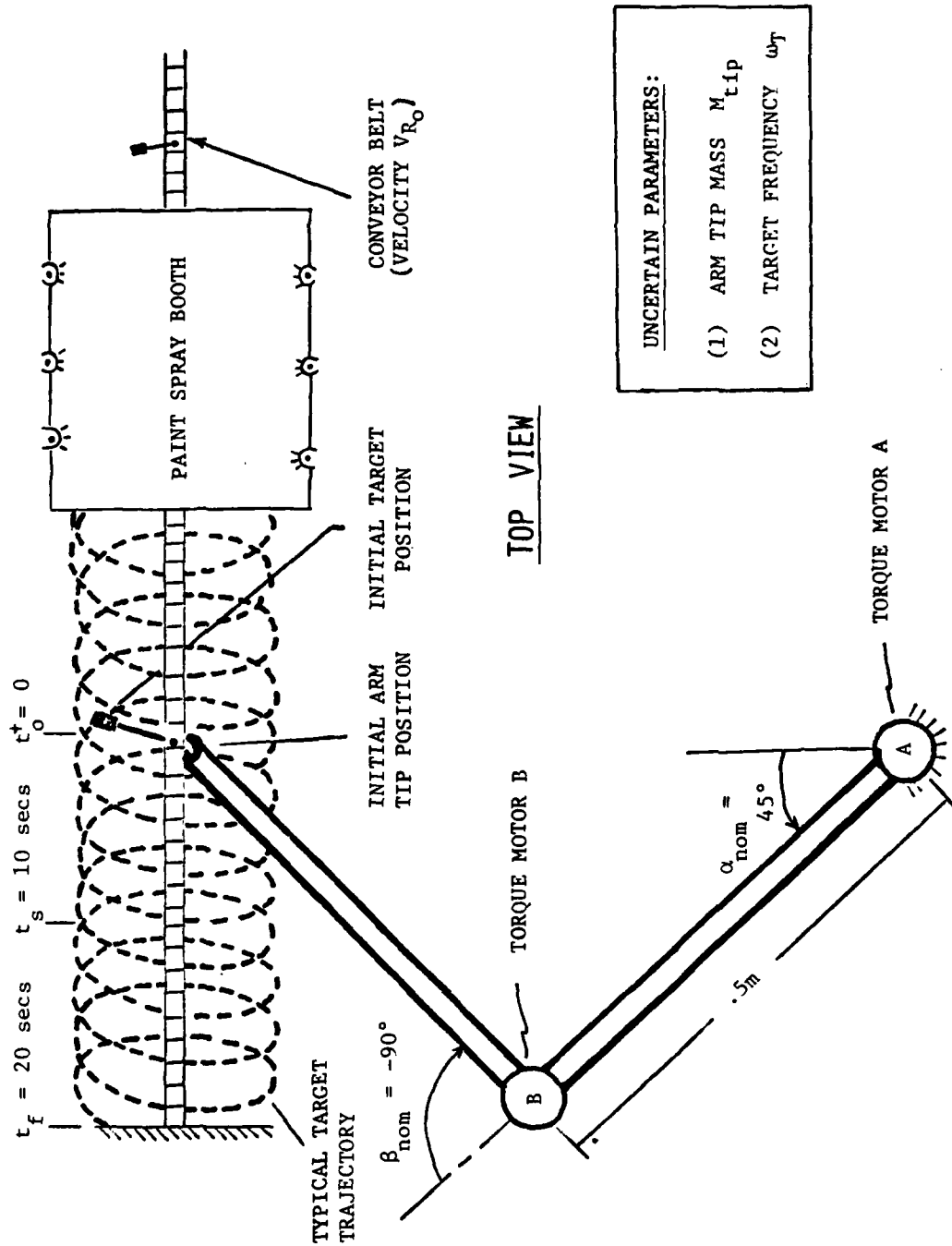


FIG. 2 TARGET TRACKING APPLICATION FOR 2L/2A ARM: PICK UP FROM PAINT SPRAY BOOTH!
 Robot arm tip to rendezvous and grasp swinging object (target) after
 $t_s = t_o^+ + 10 \text{ secs}$ but before $t_f = t_o^+ + 20 \text{ secs}$

2.1 Choice of Controller Structures

The capacity of any controller design for providing good target-tracking performance will depend to a large extent on the *structure* of the controller (i.e. specification of sensors; order and form of compensation) in addition to the numerical values specified for the unconstrained parameters (e.g. gains) of the structure.

Three separate controller structures are designed and evaluated for their effectiveness in providing good average transient and steady-state tracking performance over large v/u ranges for M_{tip} and ω_T :

- (I) NoFF: A controller featuring Proportional-Integral* output error feedback plus feedback of arm angle rates and no feedforward (Fig. 3).
- (II) FSFF: Same as (I) plus full-target-state feedforward (Fig. 4) or the near equivalent using noise-free measurements of position coordinates together with an approximate differentiation network to obtain rate coordinates (Fig. 5)
- (III) ESFF: Same as (I) plus feedforward of estimated target states given:

(a) noisy measurement of position	}	(Fig. 6)
coordinates(FF1)		
(b) noisy measurements of position		
and rate coordinates (FF2)		

Note that "Integral*", as used here, refers to a generalization of the classical " $1/s$ " integrator to a form better suited for tracking target motion consisting of a superposition of a ramp plus oscillatory motion at frequency ω_T (i.e. " $1/s^2$ " plus " $1/(s^2 + \omega_T^2)$ ").

From Fig. 3, it is seen that the I , portion of the Integral* block has a Laplace domain representation:

$$T_{eI}^*(s) = \frac{a_2(K_{I_r}s + K_{I_s})}{s^2 + a_1s + a_2} E^*(s)$$

For the case where $a_1 = 0$, it can be shown analytically that inclusion of this specific form

(sometimes referred to [3] as "rotating" or sinusoidal integral control) will guarantee zero steady-state tracking error with respect to target oscillatory motion at frequency $\sqrt{a_2}$. In addition, the rotating integral control provides robustness in the sense that it preserves the zero steady-state error property for *any* values of the arm or controller parameters (assuming the arm dynamics remain stable). If the target frequency $\omega_T = \omega_{T_{nom}}$ were invariant and well-known, then we could indeed set $a_1 = 0$, $a_2 = \omega_{T_{nom}}$ and be assured of perfect steady-state tracking. However, ω_T is one of the variable parameters in this design problem. Hence, we allow both a_1 and a_2 to be free parameters to be decided upon by an optimization process (see Section 2.3) which will account directly for the variability in ω_T .

Similarly, it is readily apparent from Fig. 3 that the Laplace representation of the I_r sub-block is simply:

$$T_{eI_r}^i(s) = \frac{K_{I_r}}{s} E^i(s)$$

Inclusion of this integrator term in conjunction with the natural $1/s$ integration from arm tip velocity to position will guarantee zero steady-state error with respect to the ramp portion of the target motion.

For the FSFF structure, the point is made that, given a relatively noise-free measurement of a target position coordinate y_T only, an estimate of the corresponding target rate coordinate v_T can be obtained by implementation of an approximate differentiator with s-domain form:

$$\hat{V}_T(s) = \frac{Ls}{s + L} Y_T(s)$$

The above representation corresponds in the time domain to a "reduced-order observer" of target rate given a measurement of position. Since the target position measurement is assumed to be relatively noise-free, the gain L can be made very large in which case the estimate \hat{v}_T is a very good approximation to actual v_T . In this case, the performance of the controller of Fig. 5 will be almost identical to that of the ideal FSFF controller of Fig. 4. Of course, if high L is to be used, it is essential that the differentiation network (i.e. observer) be allowed to run open loop for a short time prior to $t = t_0^+$ to provide for decay of large initial transients in \hat{v}_T before any control action is taken.

It is noted that the performance obtained using FSFF represents the ideal performance attainable using either FF1 or FF2 in the absence of noise.

At the cost of providing extra sensors, the addition of feedforward compensation to the baseline NoFF structure would appear to offer a means for improving the performance without affecting the arm stability characteristics. In this report, no attempt is made to provide a rigorous mathematical demonstration of the mechanism by which feedforward compensation can beneficially affect the tracking performance (analysis of either transfer function $Y(s)/Y_T(s)$ or $E(s)/Y_T(s)$ can provide a great deal of insight into this question ...Ref. [2] and [4]). Instead, using recently developed techniques for quadratic synthesis of robust controllers for "optimal" target-tracking, the feedforward/feedback structures are designed and evaluated against the NoFF structure designed to the same criteria.

$x, y \equiv$ Arm Tip Position Coordinates
 $x_T, y_T \equiv$ Target Position Coordinates
 $\alpha, \beta \equiv$ Arm Joint Angles

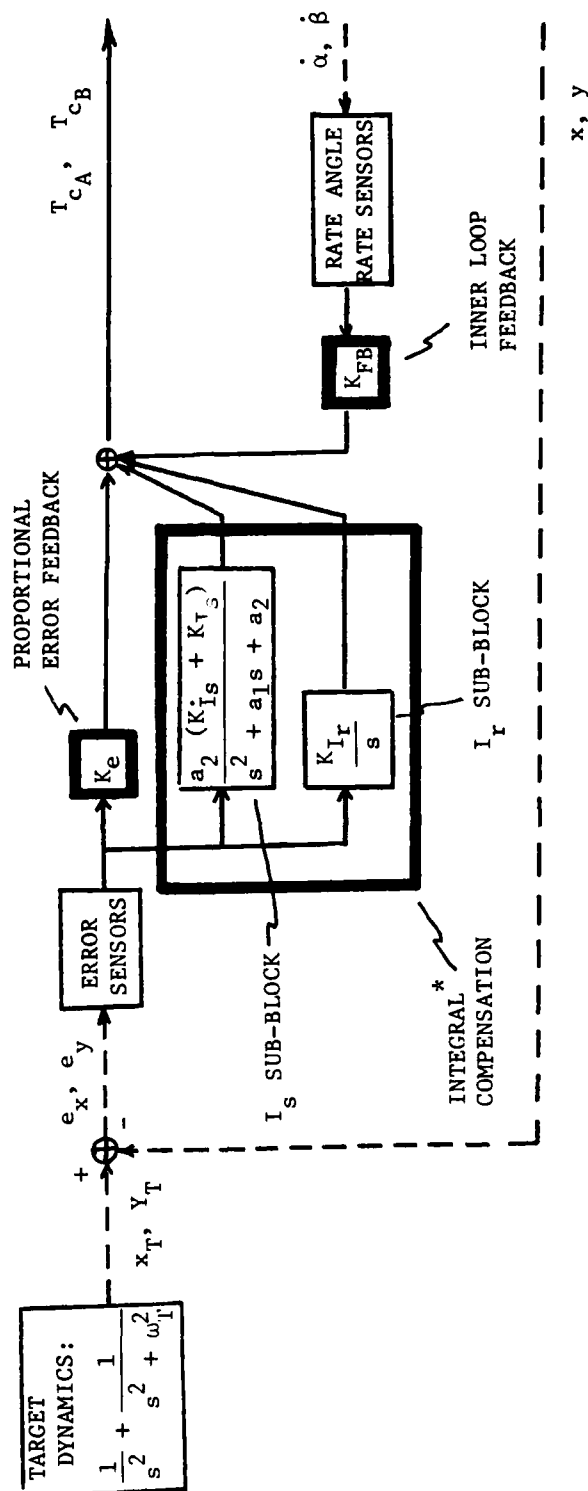


FIG. 3 CONTROLLER STRUCTURE (I): "NoFF" (NO FEEDFORWARD)
 Baseline tracking controller for 2L/2A arm of Figure 2.
 Integral compensation included for precise steady-state tracking. Controller parameters to be "optimized" using SANDY1 algorithm

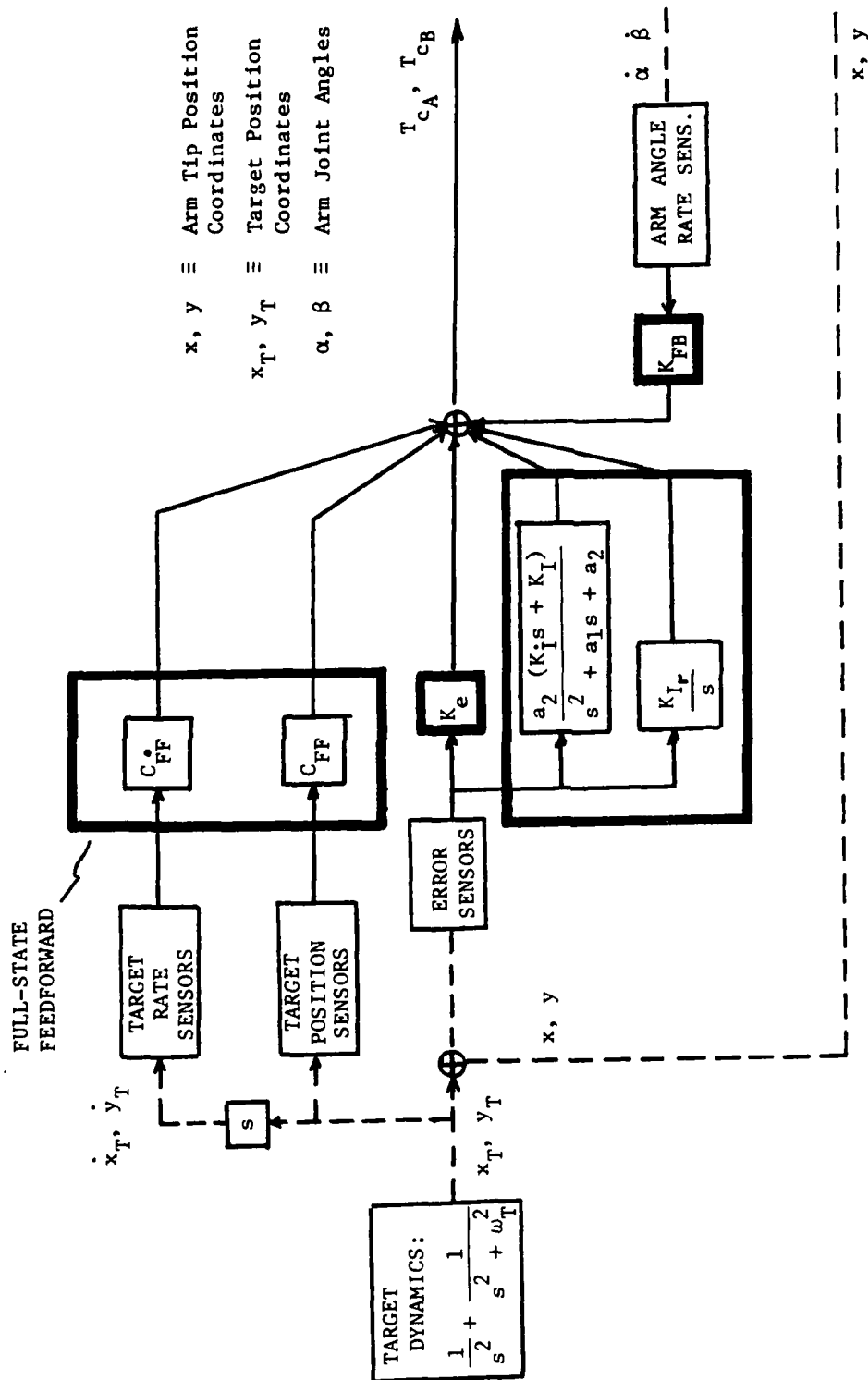


FIG. 4 CONTROLLER STRUCTURE (II): "FSFF" (FULL-STATE FEEDFORWARD)
 Baseline Controller of Fig. 3 plus feedforward of measured target position and rate coordinates. All measurements are assumed noise-free

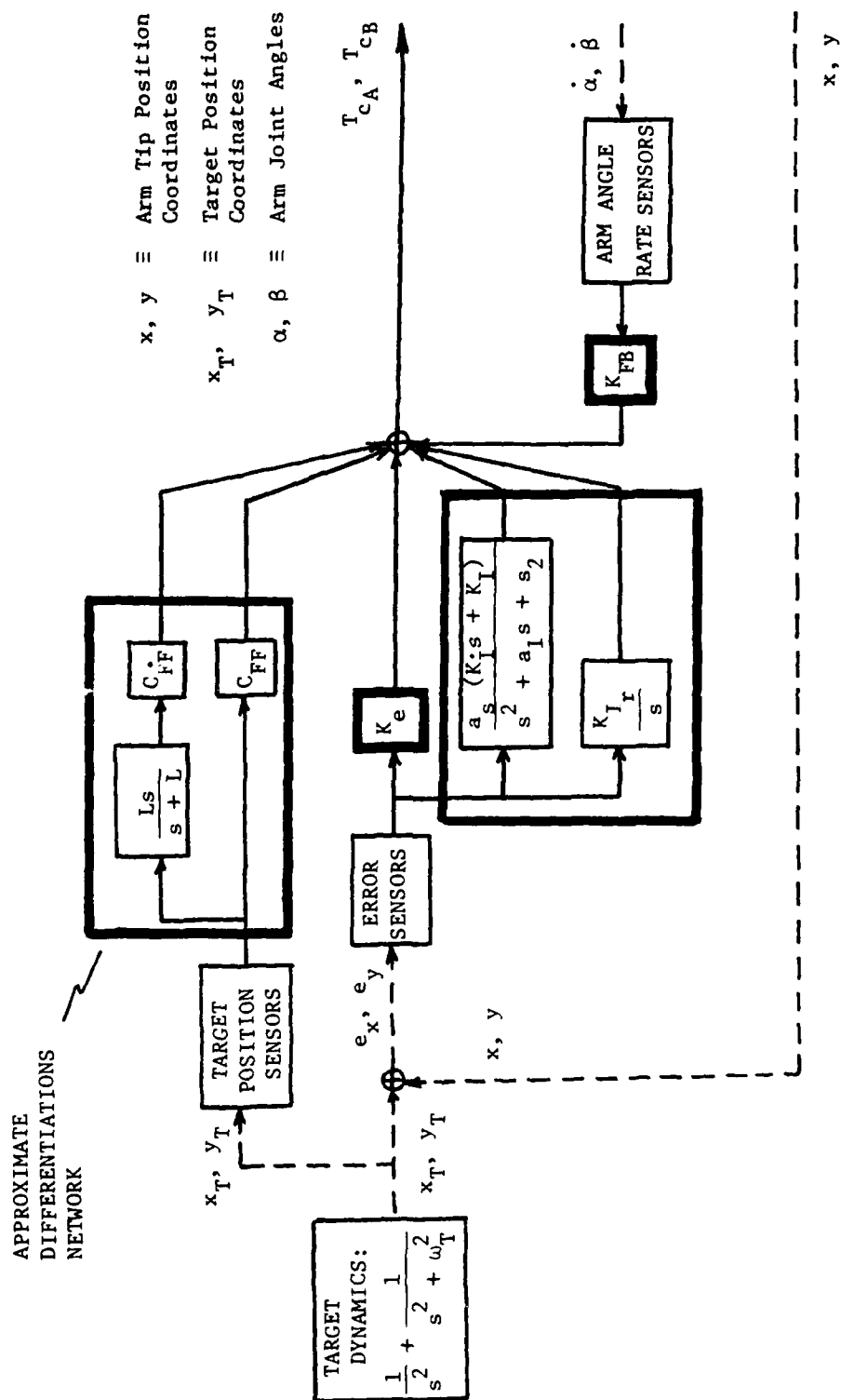


FIG. 5 NEAR EQUIVALENT TO FSFF CONTROLLER OF FIG. 4
Target position coordinate measurements assumed noise-free. Approximate differentiation network used to obtain "near perfect" estimates of target coordinates



FIG. 6. CONTROLLER STRUCTURE (III): "ESFF" (ESTIMATED STATE FEEDFORWARD)

target position and rate coordinate measurements assumed contaminated with high bandwidth noise. SANDYL algorithm used to optimize all controller parameters, including those associated with target state estimator

2.2 Choice of Performance Criteria

In order to determine the relative advantages of including feedforward of measured (and/or estimated) target states in the overall target-tracking control scheme, it is essential that each of the proposed controller structures be designed and evaluated according to some consistent performance criterion which adequately reflects the design goals stated previously. For example, this criterion might be stated in physical terms as:

PERFORMANCE CRITERION A: "Minimum average (over parameter v/u ranges) value achievable for a weighted sum of mean square transient and steady-state tracking errors without exceeding allowable limits on peak and steady-state torques"

This criterion is useful in the typical case where a specific torque motor is available and it is desired to produce the lowest errors possible without violating the torquer allowable limits. Alternatively, the primary task of the preliminary design phase may be to size the torque motor for given bounds on the tracking errors, in which case:

PERFORMANCE CRITERION B: "Minimum average value of a weighted sum of peak torque and steady-state torques required to insure that mean square transient and steady-state tracking errors do not exceed some specified bounds"

An effective synthesis tool for optimizing controller parameters according to P.C. (A) or P.C. (B) is provided by a modified version of a recently developed computer algorithm ("SANDY") for the design of robust, low-order controllers ([4] and [5]). The modified algorithm ("SANDY1") uses a non-linear programming search to minimize a newly defined quadratic performance index especially suited to the important class of target-tracking problems for which the target dynamics are characterized by one or more neutrally stable and/or unstable modes. A brief description of this algorithm is described next.

2.3 Brief Description of "SANDY1" Design Algorithm

Given linearized plant and target dynamics corresponding to parameter condition i of the form:

$$\dot{x}^i = \begin{bmatrix} \dot{x} \\ \dot{x}_r \end{bmatrix}^i = \begin{bmatrix} F & 0 \\ 0 & F_r \end{bmatrix}^i \begin{bmatrix} x \\ x_r \end{bmatrix}^i + \begin{bmatrix} G \\ 0 \end{bmatrix}^i u^i + \begin{bmatrix} \Gamma & 0 \\ 0 & \Gamma_r \end{bmatrix}^i \begin{bmatrix} w \\ w_r \end{bmatrix}^i$$

where w^i and w_r^i are zero-mean white noise sources with power spectral densities given by:

$$E \begin{bmatrix} w(t)w'(\tau) & w(t)w_r'(\tau) \\ w_r(t)w'(\tau) & w_r(t)w_r'(\tau) \end{bmatrix}^i = \begin{bmatrix} Q & 0 \\ 0 & Q_r \end{bmatrix}^i \delta(t - \tau)$$

Random initial conditions are described by the covariance matrix:

$$X_0^i = E [x_0^i x_0^{i'}]$$

The target dynamics matrix F_r may be characterized by one or more neutrally stable and/or unstable modes. However, it is assumed that these modes are "excited" only by random initial conditions.

Given a constant parameter compensator structure of the form:

$$y_s^i = H_s^i x^i + D_{su}^i u^i + D_{sw}^i w^i$$

$$u^i = D y_s^i + C z^i$$

$$\dot{z}^i = A z^i + B y_s^i$$

$$K \equiv \begin{bmatrix} D & \vdots & C \\ \dots\dots\dots \\ B & \vdots & A \end{bmatrix}$$

The SANDY1 algorithm for design of robust target-tracking controllers is based upon minimization with respect to the unconstrained elements in K of a "weighted-average" quadratic performance index of the following form (simplified form for illustrative purposes):

$$(I) \quad J^* = \sum_{i=1}^{np} \rho^i J^i$$

$$(II) \quad J^i = E \left(\lim_{t_f \rightarrow \infty} \left[\frac{1}{2t_f} \int_0^{t_f} e_{ss}^{i'} Q_{ss} e_{ss}^i + u_{ss}^{i'} R_{ss} u_{ss}^i \right] + \frac{1}{2} u_0^{i'} R_0 u_0^i \right. \\ \left. + \frac{1}{2} \int_0^{t_f} \Delta e^{i'} Q \Delta e^i + \Delta u^{i'} R \Delta u^i dt \right)$$

where,

np = total number of discrete plant/target parameter conditions

ρ^i = probability for occurrence of plant/target parameter condition i

$e^i(t)$ = tracking error vector of dimension n_o = $e_{ss}^i(t) + \Delta e^i(t) = H_T^i x_T^i - H^i x^i$
(see Fig. 7)

$u^i(t)$ = control vector of dimension $nc = u_{ss}^i(t) + \Delta u^i(t)$ (see Fig. 7)

$e_{ss}^i(t)$ = steady-state portion of tracking error vector

$u_{ss}^i(t)$ = steady-state portion of control vector

$\Delta e^i(t)$ = transient portion of tracking error vector

$\Delta u^i(t)$ = transient portion of control vector

u_0^i = initial value of control vector

t_f^* = finite time interval over which transient criteria are to be "penalized"
...selected by designer

A more compact form of J^* is obtained by use of the following definitions:

$[e_{ss}^2]^i = (no * no)$ time-averaged covariance matrix

associated with the steady-state error vector = $E \left(\lim_{t_f \rightarrow \infty} \frac{1}{t_f} \int_0^{t_f} e_{ss}^i e_{ss}^{i'} dt \right)$

$[u_{ss}^2]^i = (nc * nc)$ time-averaged covariance matrix

associated with the steady state control vector = $E \left(\lim_{t_f \rightarrow \infty} \frac{1}{t_f} \int_0^{t_f} u_{ss}^i u_{ss}^{i'} dt \right)$

$[\Delta e_m^2]^i = (no * no)$ time-averaged covariance matrix

associated with the transient error vector = $E \left(\frac{1}{t_{ss}} \int_0^{t_f^*} \Delta e^i \Delta e^{i'} dt \right)$

$[\Delta u_m^2]^i = (\text{nc} * \text{nc})$ time-averaged covariance matrix

associated with the transient control vector $= E \left(\frac{1}{t_{su}} \int_0^{t_{su}} \Delta u^i \Delta u^{i'} dt \right)$

$[u_{0m}^2]^i = (\text{nc} * \text{nc})$ covariance matrix associated with the initial control vector
 $= E (u_0 u_0')$

$t_{se} =$ arbitrary-valued dimensionalizing parameter selected by designer (e.g. set equal to desired error settling time)

$t_{su} =$ arbitrary-valued dimensionalizing parameter selected by designer (e.g. set equal to desired control settling time)

Employing the matrix trace operator together with the above definitions, we can express (I) and (II) as:

$$(III) \quad J^* = \sum_{i=1}^{np} \rho^i J^i$$

$$(IV) \quad J^i = \frac{1}{2} \text{Tr} \left(Q_{se} [e_{se,m}^2]^i + Q [\Delta e_m^2]^i + R_0 [u_{0m}^2]^i \right. \\ \left. + R_{se} [u_{se,m}^2]^i + R [\Delta u_m^2]^i \right)$$

The cost function and its gradients with respect to the unconstrained compensator parameters have been evaluated analytically ([4] and [5]) to speed convergence of the non-linear programming search for a local minimum of J^* .

The designer chooses the order and form of the compensator structure and makes an initial guess (not necessarily resulting in a stable plant for all i) for the compensator parameters. The iterative, non-linear programming search then ensues. The finite time formulation of the transient portion of the cost function was proposed [5] primarily as

a means for avoiding computational difficulties associated with an unstable initial guess for the compensator parameters.

The above form for the cost function is particularly well suited to tracking problems in which the linearized target dynamics contain neutrally stable/unstable modes. For these problems, steady-state tracking errors and control responses may occur depending upon factors such as choice of controller structure and variability of plant/target parameters. Note that a separate weighting on initial total control effort is also allowed. It has been found [4] that inclusion of this term provides a more direct means of meeting design specs for peak allowable transient control excursion. In general, the above formulation of J^* gives the designer more flexibility to trade off transient versus steady-state performance criteria so as to meet the specific target-tracking design requirements.

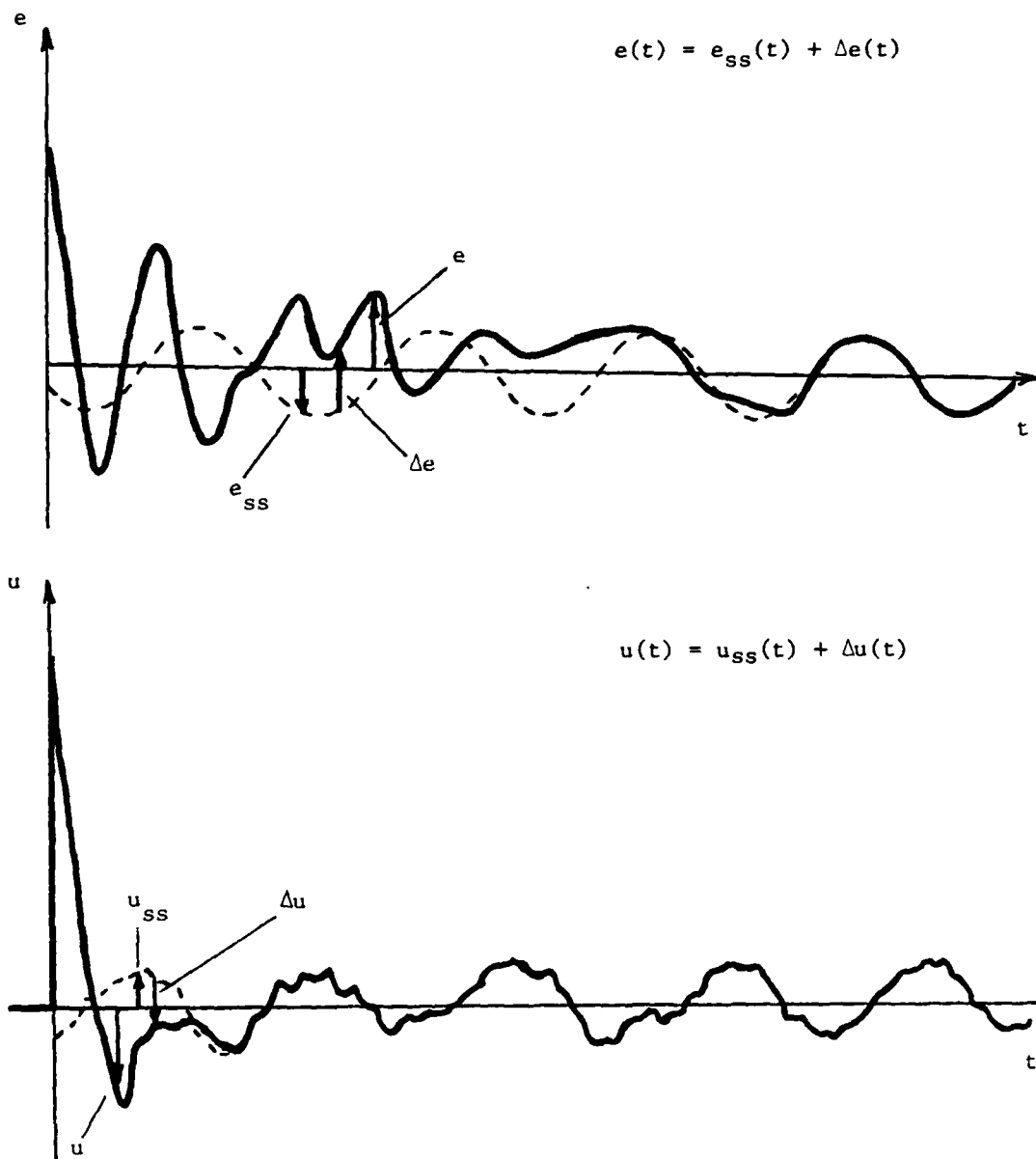


FIG. 7 ILLUSTRATION OF SANDY DEFINITIONS FOR TRANSIENT AND STEADY-STATE CRITERIA

Total tracking error and control responses are considered as superpositions of a non-decaying, steady-state component (extrapolated backwards in time) and a decaying transient component

3.0 SINGLE-LINK, SINGLE-ACTUATOR MODEL

To facilitate understanding of the important trade-offs involved in the design of robust target-tracking control logic for the 2L/2A arm, a simplified single-link, single-actuator (1L/1A) model of the problem is first considered. In this case, we consider the arm joint to be locked with $\alpha_{nom} = \beta_{nom} = 0^\circ$ and Torque Motor B inoperative (see Fig. 2). It is desired to find a control law $T_c(t)$ which causes the arm (with variable mass M_{tip} assumed concentrated in the tip) to track effectively rectilinear target motion consisting of an oscillatory component at (variable) frequency ω_r superimposed on the cable attachment point motion at constant velocity v_{T_0} .

For the 1L/1A version of the problem, we shall consider the effects of carrying out the controller designs according to P.C.(A) only in order to get a quantitative "feel" for the design trade-offs. The design and comparative evaluation of the three structures is conducted a number of times to assess the effects of increasing magnitudes of:

- (1) arm tip mass v/u range
 - (2) target frequency v/u range
 - (3) feedforward measurement noise
- (compare NoFF vs. FSFF)
- (compare NoFF vs. FF1 and FF2 for design v/u ranges)

3.1 Problem Formulation

Single Link Arm Dynamics (linearized about $\alpha_{nom} = 0^\circ$):

$$\begin{bmatrix} \dot{\alpha} \\ \ddot{\alpha} \end{bmatrix} = \begin{bmatrix} 0 & 1 \\ 0 & 0 \end{bmatrix} \begin{bmatrix} \alpha \\ \dot{\alpha} \end{bmatrix} + \begin{bmatrix} 0 \\ \frac{1}{M_{tip} \ell^2} \end{bmatrix} T_c; \quad X_0^i = \begin{bmatrix} 0 & 0 \\ 0 & 0 \end{bmatrix}$$

$$y = \ell \alpha \quad \ell = 1.0 \text{ m}$$

where X_0^i is the initial arm state covariance matrix for parameter condition i .

Target Dynamics:

$$\begin{bmatrix} \dot{y}_{T_s} \\ \dot{v}_{T_s} \\ \dot{y}_{T_r} \\ \dot{v}_{T_r} \end{bmatrix} = \begin{bmatrix} 0 & 1 & 0 & 0 \\ -\omega_T^2 & 0 & 0 & 0 \\ 0 & 0 & 0 & 1 \\ 0 & 0 & 0 & 0 \end{bmatrix} \begin{bmatrix} y_{T_s} \\ v_{T_s} \\ y_{T_r} \\ v_{T_r} \end{bmatrix}; \quad X_{T_0}^i = \begin{bmatrix} .005 & 0 & \vdots & 0 & 0 \\ 0 & .005\omega_T^2 & \vdots & 0 & 0 \\ \cdots & \cdots & \cdots & \cdots & \cdots \\ 0 & 0 & \vdots & 0 & 0 \\ 0 & 0 & \vdots & 0 & .0004 \end{bmatrix}$$

where $X_{T_0}^i$ is the initial target state covariance matrix for parameter condition i .

It is assumed that we are unable to predict the phase of the oscillatory target motion component. Thus, the upper left quadrant of $X_{T_0}^i$ involves diagonal terms only and is associated with rectilinear sinusoidal motion of rms maximum amplitude .1 m, random phase, and frequency ω_T^i . The bottom right quadrant precisely reflects the initial conditions associated with the ramp component of the target motion (i.e. $y_{T_r}(0) = 0; v_{T_r}(0) = v_{R_0} = .02$ m/sec).

Output Error:

$$e = y_{T_s} + y_{T_r} - y$$

Variable parameters for the problem are:

$$\frac{1}{1.5} \omega_{T_{nom}} \leq \omega_T^i \leq 1.5 \omega_{T_{nom}} \quad (\omega_{T_{nom}} = 2.84 \text{ rad/sec})$$

$$\frac{1}{1.5} M_{tip_{nom}} \leq M_{tip}^i \leq 1.5 M_{tip_{nom}} \quad (M_{tip_{nom}} = 1.25 \text{ kg})$$

3.2 Compensator Descriptions

(I) NoFF (No Feedforward):

$$T_c = T_c^* = K_e e + [K_{I_1} \quad K_{I_2}] \begin{bmatrix} z_{I_1} \\ \dot{z}_{I_1} \end{bmatrix} + K_{I_1} z_{I_1} + K_{\dot{a}} \dot{a}$$

where,

$$\begin{bmatrix} \dot{z}_{I_1} \\ \ddot{z}_{I_1} \end{bmatrix} = \begin{bmatrix} 0 & 1 \\ -a_2 & -a_1 \end{bmatrix} \begin{bmatrix} z_{I_1} \\ \dot{z}_{I_1} \end{bmatrix} + \begin{bmatrix} 0 \\ a_2 \end{bmatrix} e^i \quad \dot{z}_{I_1}^i = e$$

Free parameters for optimization: $K_e, K_{I_1}, K_{I_2}, K_{I_1}, K_{\dot{a}}, a_1, a_2$

(II) FSFF (Full State Feedforward):

$$T_c = T_c^* + [C_{y_1} \quad C_{v_1} \quad C_{y_2} \quad C_{v_2}] \begin{bmatrix} y_{T_1} \\ v_{T_1} \\ y_{T_2} \\ v_{T_2} \end{bmatrix}$$

Free parameters for optimization: Same as for (I) plus: $C_{y_1}, C_{v_1}, C_{y_2}, C_{v_2}$

(III) ESFF (Estimated State Feedforward):

$$T_c = T_c^* + [C_{y_1} \quad C_{v_1} \quad C_{y_2} \quad C_{v_2}] \begin{bmatrix} \hat{y}_{T_1} \\ \hat{v}_{T_1} \\ \hat{y}_{T_2} \\ \hat{v}_{T_2} \end{bmatrix}$$

where,

$$\text{(a) FF1: } \begin{bmatrix} \dot{\hat{y}}_{T_s} \\ \dot{\hat{v}}_{T_s} \\ \dot{\hat{y}}_{T_r} \\ \dot{\hat{v}}_{T_r} \end{bmatrix} = \begin{bmatrix} 0 & 1 & 0 & 0 \\ -\omega_{T_{nom}}^2 & 0 & 0 & 0 \\ 0 & 0 & 0 & 1 \\ 0 & 0 & 0 & 0 \end{bmatrix} \begin{bmatrix} \hat{y}_{T_s} \\ \hat{v}_{T_s} \\ \hat{y}_{T_r} \\ \hat{v}_{T_r} \end{bmatrix} + \begin{bmatrix} K_{s,1} & 0 \\ K_{s,2} & 0 \\ 0 & K_{r,1} \\ 0 & K_{r,2} \end{bmatrix} \begin{bmatrix} z_1 - y_{T_s} \\ z_3 - y_{T_r} \end{bmatrix}$$

$$\text{(b) FF2: } \begin{bmatrix} \dot{\hat{y}}_{T_s} \\ \dot{\hat{v}}_{T_s} \\ \dot{\hat{y}}_{T_r} \\ \dot{\hat{v}}_{T_r} \end{bmatrix} = \begin{bmatrix} 0 & 1 & 0 & 0 \\ -\omega_{T_{nom}}^2 & 0 & 0 & 0 \\ 0 & 0 & 0 & 1 \\ 0 & 0 & 0 & 0 \end{bmatrix} \begin{bmatrix} \hat{y}_{T_s} \\ \hat{v}_{T_s} \\ \hat{y}_{T_r} \\ \hat{v}_{T_r} \end{bmatrix} + \begin{bmatrix} K_{s,11} & K_{s,12} & 0 & 0 \\ K_{s,21} & K_{s,22} & 0 & 0 \\ 0 & 0 & K_{r,11} & K_{r,12} \\ 0 & 0 & K_{r,21} & K_{r,22} \end{bmatrix} \begin{bmatrix} z_1 - \hat{y}_{T_s} \\ z_2 - \hat{v}_{T_s} \\ z_3 - \hat{y}_{T_r} \\ z_4 - \hat{v}_{T_r} \end{bmatrix}$$

where

$$z_1 = y_{T_s} + \nu_1$$

$$z_2 = v_{T_s} + \nu_2$$

$$z_3 = y_{T_r} + \nu_3$$

$$z_4 = v_{T_r} + \nu_4$$

Each noise input ν_i is assumed to be exponentially correlated with variance ν_{ff}^2 and correlation time $T = .005$ secs. Since this represents a relatively short interval compared with anticipated correlation times for the target motion, for analytic convenience we shall model¹ each ν_i as a white noise source with power spectral density Q_{ff} :

$$E(\nu_i(t) \nu_j(\tau)) = Q_{ff} \delta_{ij} (t - \tau)$$

$$Q_{ff} = 2T \nu_{ff}^2 = .01 \nu_{ff}^2$$

(rms intensity ν_{ff} will be a design parameter)

¹ see [6] for more complete explanation.

Minimal realization forms of (III)-a and (III)-b are given by:

$$T_c = T_c^* + \begin{bmatrix} \hat{C}_y & \hat{C}_v & \hat{C}_y & \hat{C}_v \end{bmatrix} \begin{bmatrix} \hat{z}_{s1} \\ \hat{z}_{s2} \\ \hat{z}_{r1} \\ \hat{z}_{r2} \end{bmatrix}$$

where,

$$\begin{array}{l} \text{(a)} \\ \text{FF1:} \end{array} \begin{bmatrix} \dot{\hat{z}}_{s1} \\ \dot{\hat{z}}_{s2} \\ \dot{\hat{z}}_{r1} \\ \dot{\hat{z}}_{r2} \end{bmatrix} = \begin{bmatrix} 0 & 1 & 0 & 0 \\ -a_{T_{s2}} & -a_{T_{s1}} & 0 & 0 \\ 0 & 0 & 0 & 1 \\ 0 & 0 & -a_{T_{r2}} & -a_{T_{r1}} \end{bmatrix} \begin{bmatrix} \hat{z}_{s1} \\ \hat{z}_{s2} \\ \hat{z}_{r1} \\ \hat{z}_{r2} \end{bmatrix} + \begin{bmatrix} 0 & 0 \\ a_{T_{s2}} & 0 \\ 0 & 0 \\ 0 & a_{T_{r2}} \end{bmatrix} \begin{bmatrix} z_1 \\ z_3 \end{bmatrix}$$

Free Parameters for Optimization: Same as for (I) plus: \hat{C}_y , \hat{C}_v , \hat{C}_y ,
 \hat{C}_v , $a_{T_{s1}}$, $a_{T_{s2}}$, $a_{T_{r1}}$, $a_{T_{r2}}$

$$\begin{array}{l} \text{(b)} \\ \text{FF2:} \end{array} \begin{bmatrix} \dot{\hat{z}}_{s1} \\ \dot{\hat{z}}_{s2} \\ \dot{\hat{z}}_{r1} \\ \dot{\hat{z}}_{r2} \end{bmatrix} = \begin{bmatrix} 0 & 1 & 0 & 0 \\ -a_{T_{s2}} & -a_{T_{s1}} & 0 & 0 \\ 0 & 0 & 0 & 1 \\ 0 & 0 & -a_{T_{r2}} & -a_{T_{r1}} \end{bmatrix} \begin{bmatrix} \hat{z}_{s1} \\ \hat{z}_{s2} \\ \hat{z}_{r1} \\ \hat{z}_{r2} \end{bmatrix} + \begin{bmatrix} 0 & b_{T_{s1}} & 0 & 0 \\ a_{T_{s2}} & b_{T_{s2}} & 0 & 0 \\ 0 & 0 & 0 & b_{T_{r1}} \\ 0 & 0 & a_{T_{r2}} & b_{T_{r1}} \end{bmatrix} \begin{bmatrix} z_1 \\ z_2 \\ z_3 \\ z_4 \end{bmatrix}$$

Free parameters for optimization: Same as for (III)-a plus: $b_{T_{s1}}$, $b_{T_{s2}}$, $b_{T_{r1}}$, b_{r2}

3.3 Controller Design and Performance Criteria

A performance criterion is now defined that reflects the design goals discussed in Section 2.0.

P.C.(A): Minimize a weighted sum of mean square transient and steady-state errors averaged over the np parameter conditions

$$\overline{e^{2^*}} \equiv \frac{\sum_{i=1}^{np} e^{2^*i}}{np}; \quad e^{2^*i} \equiv q_{ss} e_{ss,m}^{2^*i} + q \Delta e_m^{2^*i}$$

subject to constraints on the peak and steady-state control effort:

$$(*) \quad \max |T_c^i(t)| \leq 15 \text{ N-m} \quad (i = 1, np; t = 0, t_f)$$

$$T_{c,ss,m} \equiv \sqrt{\frac{\sum_{i=1}^{np} T_{c,ss,m}^{2^*i}}{np}} \leq 3 \text{ N-m}$$

The weighting parameters q_{ss} and q are chosen by the designer (on a trial and error basis) to provide a good balance between the "optimal" values of the (averaged) mean square steady-state and transient errors.

As a convenient approximation to this performance criterion, we define a quadratic cost function as follows:

$$J^* \equiv \sum_{i=1}^{np} \rho^i J^i$$

$$J^i \equiv q_{ss} e_{ss,m}^{2^*i} + q \Delta e_m^{2^*i} + r_o T_{c,om}^{2^*i} + r \Delta T_{c,m}^{2^*i} + r_{ss} T_{c,ss,m}^{2^*i}$$

A large value (i.e. 500 secs) was chosen for the finite time interval t_f^* associated with the transient terms $\Delta e_m^{2^*i}$ and $\Delta T_{c,m}^{2^*i}$ to ensure that the solution for minimization of J^* resulted in stable closed loop dynamics (see [4] for more detailed discussion). The dimensionalizing parameters t_{ss} and t_{ss} used in the definitions for the transient terms (see Section 2.3) were set equal to 10 secs and 1 sec respectively. In general, the actual peak control criterion $\max |T_c^i(t)|$ is a rather complicated non-quadratic function of

the independent controller parameters. As a convenient quadratic "surrogate" for this parameter, a weighted sum of the initial control excursion squared ($T_{c,m}^{2'}$) and the mean square transient control effort ($\Delta T_{c,m}^{2'}$) is used in the above definition of J^* .

For the selected error term weighting parameters $q_{..}$ and q , the control term weighting parameters $r, r_0, r_{..}$ are varied in a trial and error fashion by the designer until the corresponding solution for minimization of J^* meets the following constraints:

$$\text{quadratic "surrogates" for (*)} \quad \begin{cases} \overline{\Delta T_{c,m}^2} \leq 4(N-m)^2 \\ \overline{T_{c,m}^2} \leq 100(N-m)^2 \\ \overline{T_{c,ss,m}^2} \leq 4(N-m)^2 \end{cases}$$

The numerical bound on initial control excursion is based on anticipation that the optimal control strategy for each controller structure will call for large torque early on in response to initial error, initial error rate, etc., gradually tapering off to the steady-state oscillatory condition. Assuming that the maximum total control excursion occurs at $t = 0^+$, we desire to limit the average magnitude of this excursion to be less than or equal to the torque motor peak allowable (15 N-m) divided by a safety-factor of 1.5 to account for variability of the initial error and error rate magnitudes. Squaring this reduced allowable we arrive at the upper bound of $100(N-m)^2$ for $T_{c,m}^{2'}$. Similarly, a 1.5 factor was applied to the torque motor rms continuous limit of 3 N-m to arrive at a reduced allowable for the *average rms continuous* (i.e. steady-state) torque. Squaring this reduced allowable, we arrive at the upper bound of $4(N-m)^2$ for $\overline{T_{c,ss,m}^2}$.

Ideally, the upper bound on mean square transient control effort should be chosen equal to a value η_u which is "just small enough" to ensure that the optimal control law will not call for any control excursions of magnitude greater than 15 N-m for all times greater than $t = t_0^+$. In general, the exact value of η_u necessary to achieve this is not known by the designer a priori and, in fact, will depend upon the controller structure being optimized. To avoid additional trial and error procedures which would be required to determine η_u accurately, a value of $4.0(N-m)^2$ was assumed and used in the design of

each controller structure. This choice seemed to consistently result in controller designs that did not violate the peak torque constraints for t greater than t_0^+ yet allowed for reasonably fast decay of transient errors.

It is likely that many different combinations $(r, r_0, r_{..})$ will result in corresponding control law design solutions that satisfy the above *inequality* relationships. Thus, to ensure uniqueness of the solution, we further require that each control term weighting parameter be zero unless the corresponding constraint (i), (ii), or (iii) is active (i.e. the *equality* relation holds).

It can be demonstrated that the solution which meets the above criteria is "optimal" in the sense that the resulting value of $\overline{e^2}$ is the *minimum* value attainable subject to the numerical constraints placed on the control terms.

4.0 DESIGN RESULTS FOR 1L/1A MODEL

4.1 Nominal Parameter Case (NoFF vs. FSFF)

For the case of nominal arm/target dynamic parameters and initial conditions, SANDY1 was used to synthesize "optimal" controller parameters for the NoFF and FSFF controller structures according to P.C.(A) with $q = 80$ and $q_{..} = 50000$. Controller parameter values, closed loop eigenvalues and performance data are summarized in Table (1). Observe that the optimized " I_s " compensator sub-block contains a duplicate of the oscillatory portion of the nominal target dynamics for both controllers, thus ensuring zero steady-state error with respect to target oscillatory motion at frequency $\omega_{r_{nom}} = \sqrt{8.07}$ rad/sec. Similarly, as discussed earlier, it is readily apparent that inclusion of the $1/s$ integrator term in conjunction with the natural $1/s$ integration from arm tip velocity to position provides a model of the ramp portion of the target motion; hence, zero steady-state error with respect to the target ramp motion is also preserved.

Since the " I_s " and " I_r " sub-blocks insure zero steady-state error for the case of nominal target dynamic parameters, the only effect of feedforward appears in the transient tracking response. As shown in Table (1), the percent improvement in root mean square transient tracking error Δe_m for the same control effort offered by feedforward of all target states is substantial (42% reduction from NoFF to FSFF).

To provide a more direct comparison of the transient response characteristics of the three optimized controllers for nominal parameters, Figs. 8 and 9 show simulated time responses for one possible set of initial conditions (i.e. arm tip initially at rest at y_{R_0} ; target at max amplitude (.1 m) and beginning "forward" swing). Note the much lower undershoot and settling time obtained with feedforward (Fig. 8) for approximately the same control effort (Fig. 9).

TABLE 1
CLOSED LOOP DATA FOR OPTIMIZED 1L/1A CONTROLLERS
DESIGNED FOR NOMINAL PARAMETER CASE

Controller Parameter Values	Controller (I) NoFF	Controller (II) FSFF
K_e K_{I_s} K_{i_s} K_{I_r} K_{θ}	100.86 -55.55 17.86 29.28 -15.04	139.01 -7.49 10.29 14.50 -18.12
$I_s^* \equiv \begin{bmatrix} 0 & 1 \\ -a_2 & -a_1 \end{bmatrix}$	$\begin{bmatrix} 0 & 1 \\ -8.07 & 0 \end{bmatrix}$	$\begin{bmatrix} 0 & 1 \\ -8.07 & 0 \end{bmatrix}$
C_{y_s} C_{v_s} C_{y_r} C_{v_r}	- - - -	-16.82 17.83 0 17.78
Closed Loop Eigenvalues	$-4.22 \pm j5.99$ $-.785 \pm j1.08$ $-.97$	$-6.83 \pm j7.29$ $-.34 \pm j2.86$ $-.113$
Performance Data		
Δe_m (m) e_{ssm} (m) ΔT_{cm}^2 (N-m) ² T_{com}^2 (N-m) ² T_{ssm}^2 (N-m) ²	.012 0 3.97 50.9 .51	.007 0 3.92 88 .51

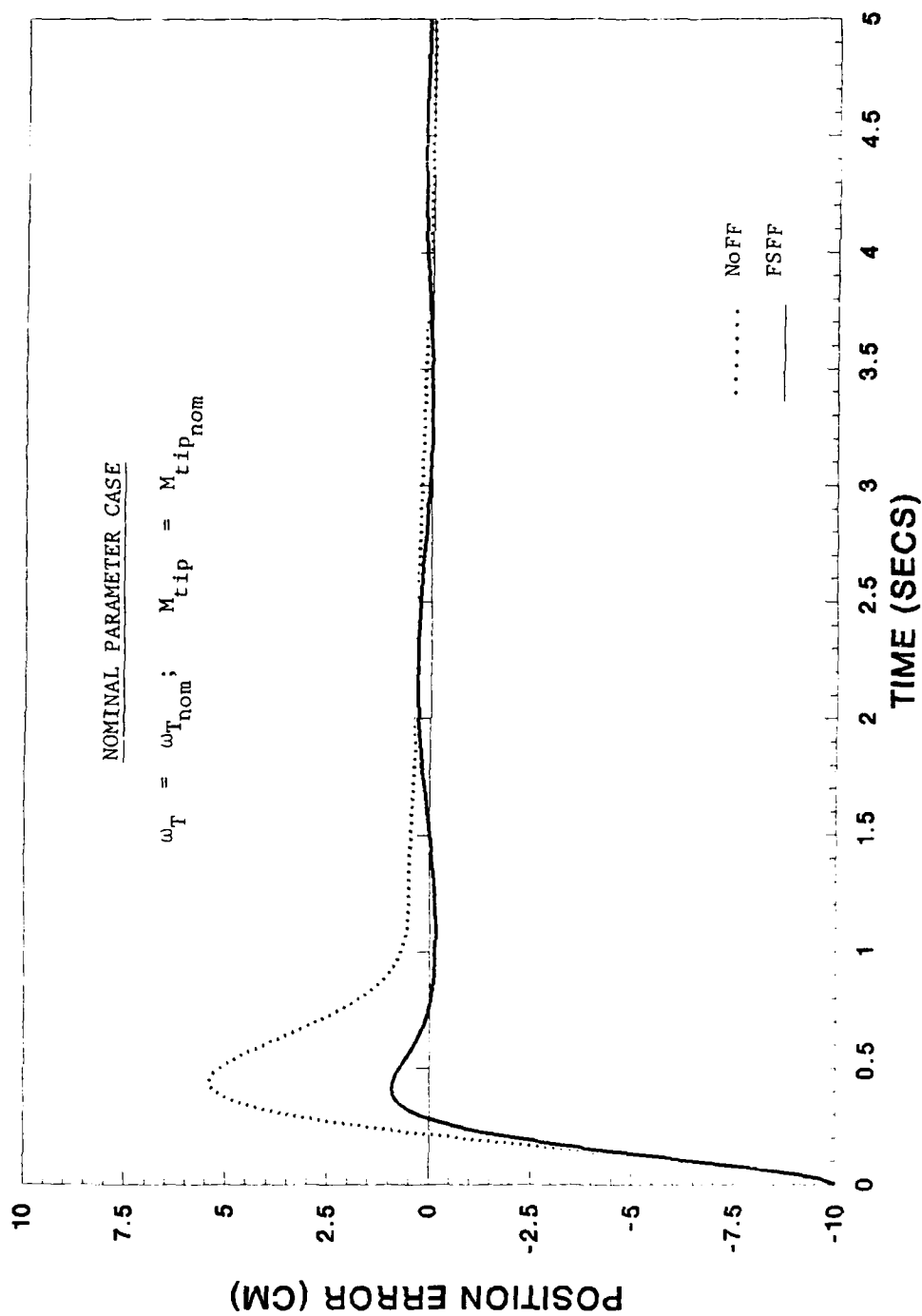


FIG. 8 POSITION ERROR TIME HISTORIES: NoFF vs FSFF NOMINAL PARAMETERS CASE
Inclusion of feedforward significantly reduces transient error over-shoot. For nominal parameters, zero steady-state error will result with both controllers

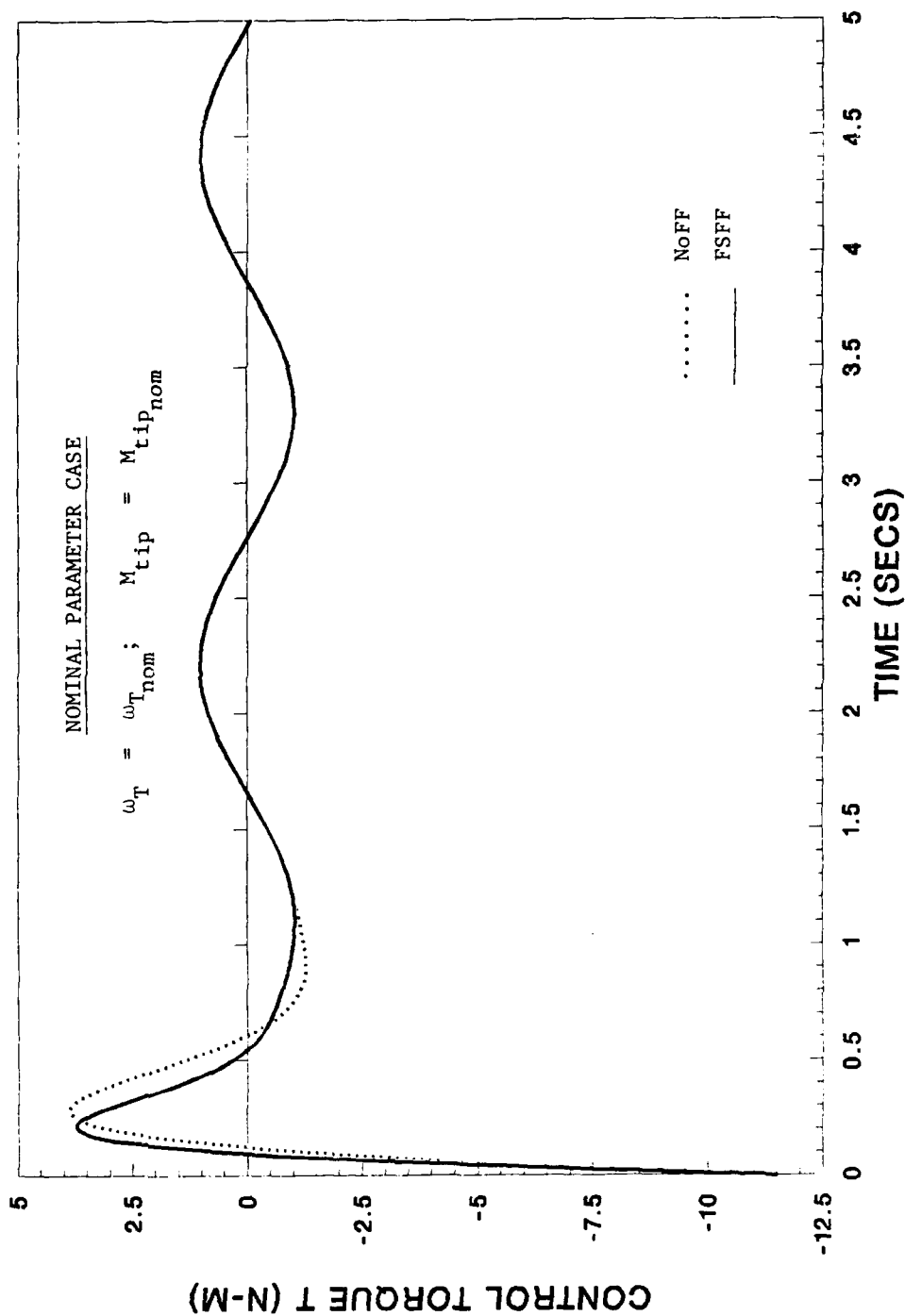


FIG. 9 CONTROL TORQUE TIME HISTORIES: NoFF vs FSFF NOMINAL PARAMETERS CASE
Control torque histories required to produce the tracking error response of Fig. 8. Note the faster transient control response obtained with feedforward, resulting directly in lower transient tracking errors

4.2 Effect of Arm Tip Mass Variations (NoFF vs. ESFF at $\omega_T = \omega_{Tnom}$)

As discussed previously, inclusion of the "I" block in all three controller structures insures zero steady-state error with respect to nominal target motion despite arm parameter (e.g. tip mass) variations. Hence, again we anticipate the effects of feedforward control to appear only in the transient response characteristics. To explore the capacity of feedforward to provide good average tracking behavior over wide ranges of tip mass variations, Controllers (I) and (II) were "re-optimized" for increasing values of a tip mass variability range factor a_m , defined by:

$$\frac{1}{a_m} M_{tip_{nom}} \leq M_{tip} \leq a_m M_{tip_{nom}}$$

For each integer value of a_m ($1 \leq a_m \leq 4$), SANDY1 was used to optimize parameters of both controllers assuming $n_p = 3$ corresponding to three discrete arm parameter conditions:

$$(i) M_{tip} = M_{tip_{min}} = \frac{1}{a_m} M_{tip_{nom}} \quad (\rho = .3333)$$

$$(ii) M_{tip} = M_{tip_{nom}} \quad (\rho = .3333)$$

$$(iii) M_{tip} = M_{tip_{max}} = a_m M_{tip_{nom}} \quad (\rho = .3333)$$

Figure 11 shows the comparative average performance over the three tip mass conditions. It is clear that, as tip mass variability range increases, the FSFF controller demonstrates an increasing improvement in average transient tracking performance. For a design value of $a_m = 1.5$, full state feedforward offers a 35% reduction in average root mean square transient error $\overline{\Delta e_m}$ for the same control effort.

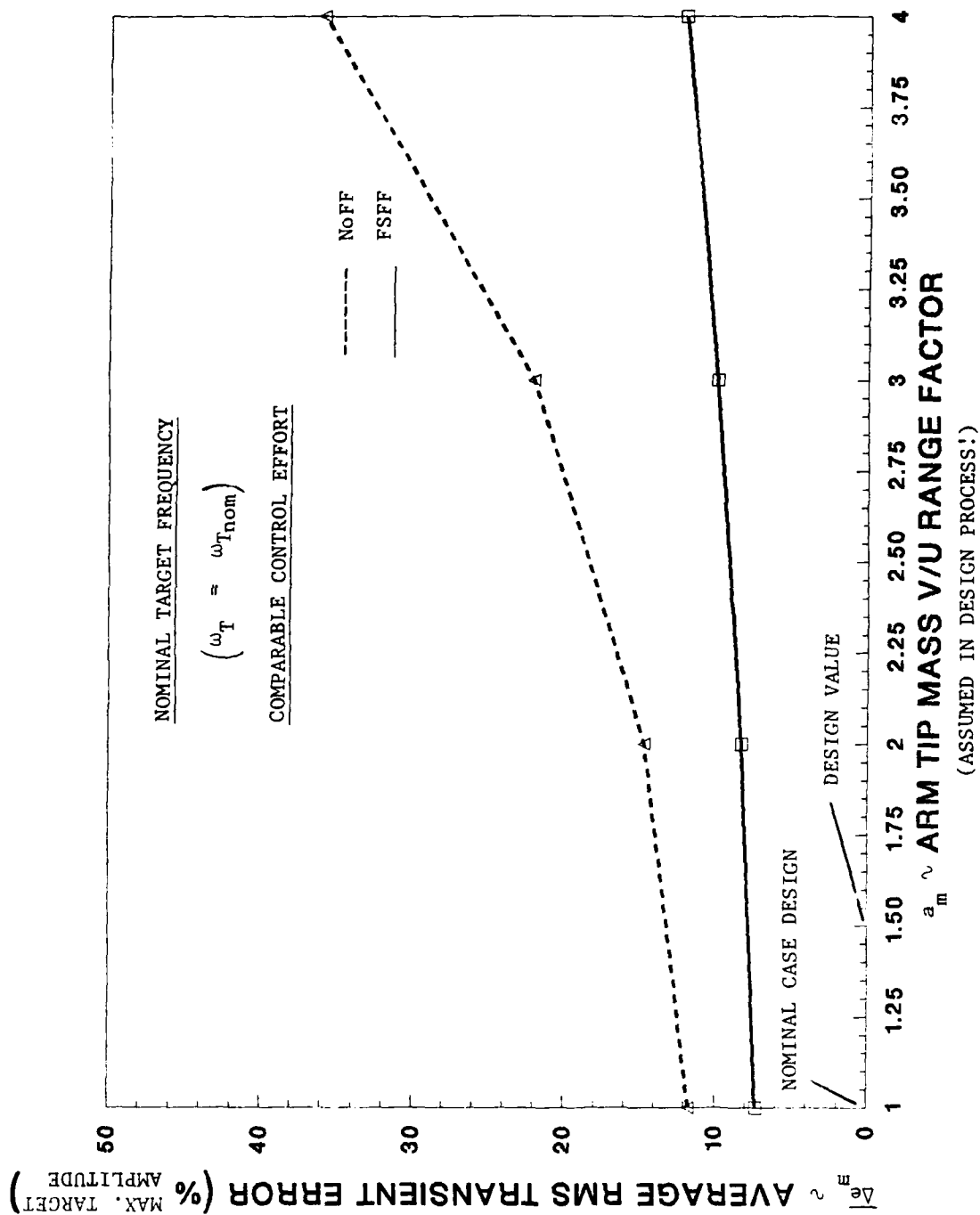


FIG. 10 EFFECT OF ARM TIP MASS VARIABILITY ON TRANSIENT TRACKING: NoFF vs FSFF
 As tip mass variability/uncertainty range assumed in the design process increases, relative improvement in transient tracking accuracy (for same control effort) obtained with feedforward also increases

4.3 Effect of Target Frequency Variations (NoFF vs. FSFF at $M_{tip} = M_{tip_{nom}}$)

If variability exists in the target frequency, it is not possible to specify a unique " I_c " control sub-block which will insure zero steady-state error with respect to target oscillatory motion over the entire variability range. Thus, the feedforward compensation may affect steady-state as well as transient error behavior. Figures 11-12 present performance results obtained for both controller structures, each optimized according to P.C. (A) with $q = 80$ and $q_{ss} = 50000$ for increasing values of a target frequency variability factor a_{ω_T} , defined in the same manner as a_m . Once again, the advantages of the FSFF controller are evident, especially as a_{ω_T} becomes large in which case *both* transient and steady-state rms errors (averaged) are seen to be significantly lower than for the optimized NoFF controller. These results may seem somewhat surprising in view of the sometimes-expressed notion that good feedforward control can be designed only if the target dynamics are fixed and well-known. Apparently, by accounting for several discrete possibilities for the target frequency in the design process (as was done here), the optimization process produces a "robust" set of feedforward parameters which improves the *average* tracking performance over the target frequency v/u range. It would seem that, when optimizing the average tracking performance for any given range of target frequency v/u, inclusion of independent feedforward parameters should *always* be beneficial since additional degrees-of-freedom are then available for improving the performance.

4.4 Effect of Noise in Feedforward Measurement(s) (NoFF vs. ESFF at $a_{\omega_T} = a_m = 1.5$)

Results up to this point indicate that the inclusion of optimally designed feedforward compensation in the overall target-tracking control scheme does indeed offer some significant performance payoffs, especially for large target frequency variability ranges. However, the detrimental effect of random noise in the feedforward measurement(s), neglected up to now, must also be considered. We should expect that, as the noise levels in the feedforward measurement(s) increase relative to the feedback measurement noise, the optimized solution will call for lower feedforward gains and rely more on the feedback-only portion of the controller structure at the expense of tracking accuracy. To explore this hypothesis in a quantitative fashion, we now consider the effect of increasing levels

of random (i.e. "white") noise in the target measurement(s). For the ESFF controllers FF1 and FF2, optimal parameters are synthesized by SANDY1 assuming design values of 1.5 for both a_{ω_T} and a_m , and accounting for white noise sources of equal power spectral density $Q_{ff} = 2T \nu_{ff}^2$ (see Section 3.2) in each of the target state measurements, where T is taken to be .005 secs and ν_{ff} is the parameter to be varied. Five discrete parameter conditions were defined to bracket the design ranges for the variable parameters. These are:

Cond #	Probability ρ^i	M_{tip} (kg)	ω_T (rad/sec)
1	.3	1.25	2.84
2	.175	.625	1.89
3	.175	.625	4.26
4	.175	2.5	1.89
5	.175	2.5	4.26

For each controller design, cost function weighting parameters $q_{..}$ and q were chosen on a trial and error basis to strike a good balance between the "optimal" steady-state and transient error characteristics. Also, in the optimization process it was assumed¹ that the target state estimator had been running open loop for a short time prior to $t = t_0^+$ so as to attenuate the effects of large initial estimator errors on the control effort.

Figures 13 and 14 show the resulting optimal transient and steady-state error performance (for approximately the same control effort) of the ESFF controllers versus the NoFF controller as a function of the design value for the feedforward measurement white noise intensity. Since the NoFF controller does not use the feedforward measurements, its performance is obviously constant for increasing ν_{ff} .² With the FF1 controller, the transient and steady-state tracking accuracies are seen to degrade significantly relative to that of NoFF as the design level of measurement noise increases. Using the additional measurements of target rate coordinates (FF2 controller) appears to buy considerable

¹ this involved recalculation of initial vlaues for the feedforward compensator states to be used as part of the input to SANDY1

² expressed as a percentage of the maximum expected target position amplitude (= 10 cm)

improvement in both transient and steady-state tracking accuracies, especially at higher design levels of measurement noise. At a design noise level of $\nu_{ff} = 5\%$, the average rms transient and steady-state errors with FF1 are, respectively, 30% and 38% less than for NoFF. By comparison, FF2 is seen to provide more dramatic reductions of 40% in rms transient error and 85% in rms steady-state error.

Controller parameters and average closed loop performance data for each structure designed for the five parameter conditions and $\nu_{ff} = 5\%$ are summarized in Table (2).

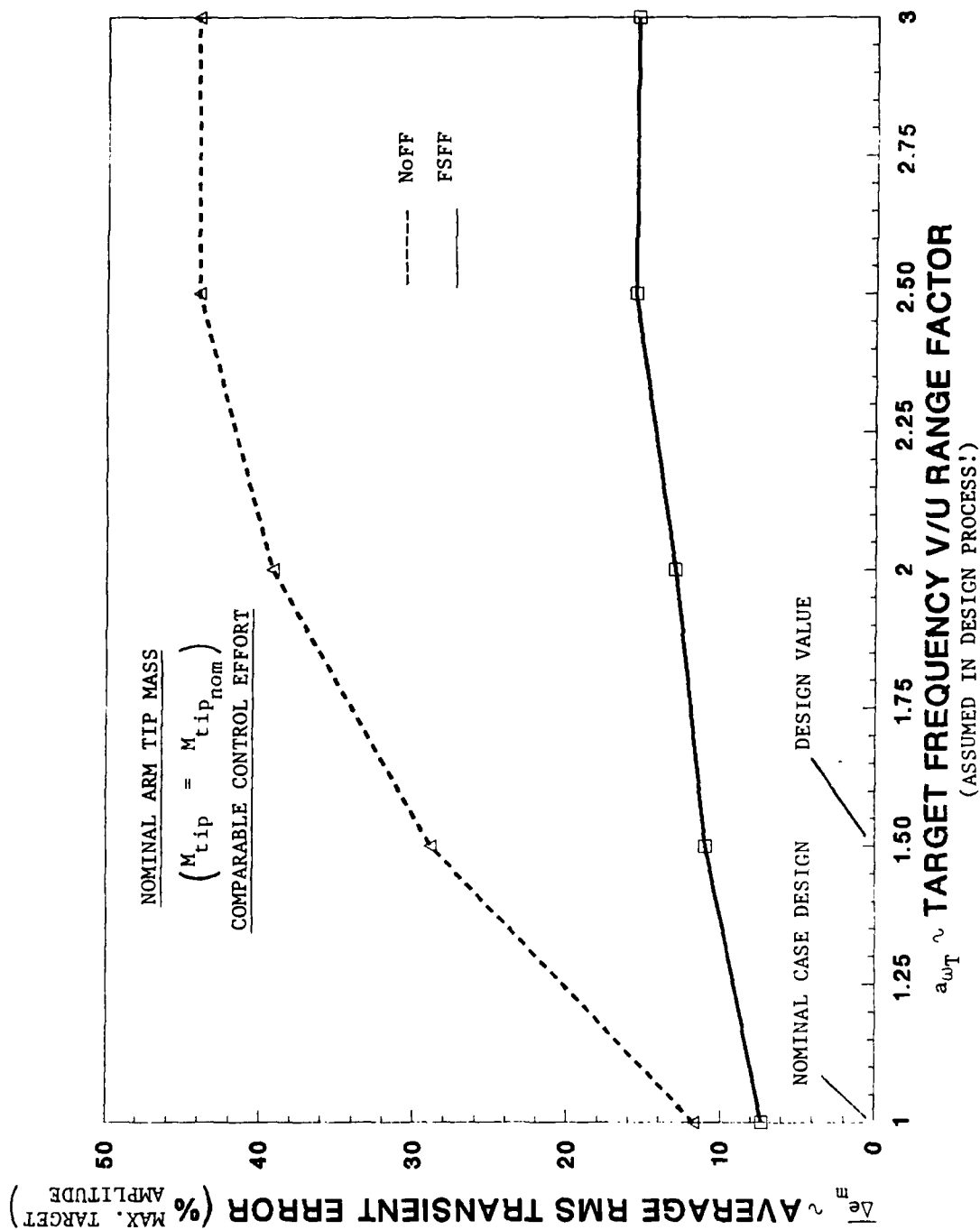


FIG. 11 EFFECT OF TARGET FREQUENCY VARIABILITY ON TRANSIENT TRACKING: NoFF vs FSFF
 As target frequency variability/uncertainty range assumed in the design process increases, relative improvement in transient tracking accuracy (for some control effort) obtained with feedforward also increases

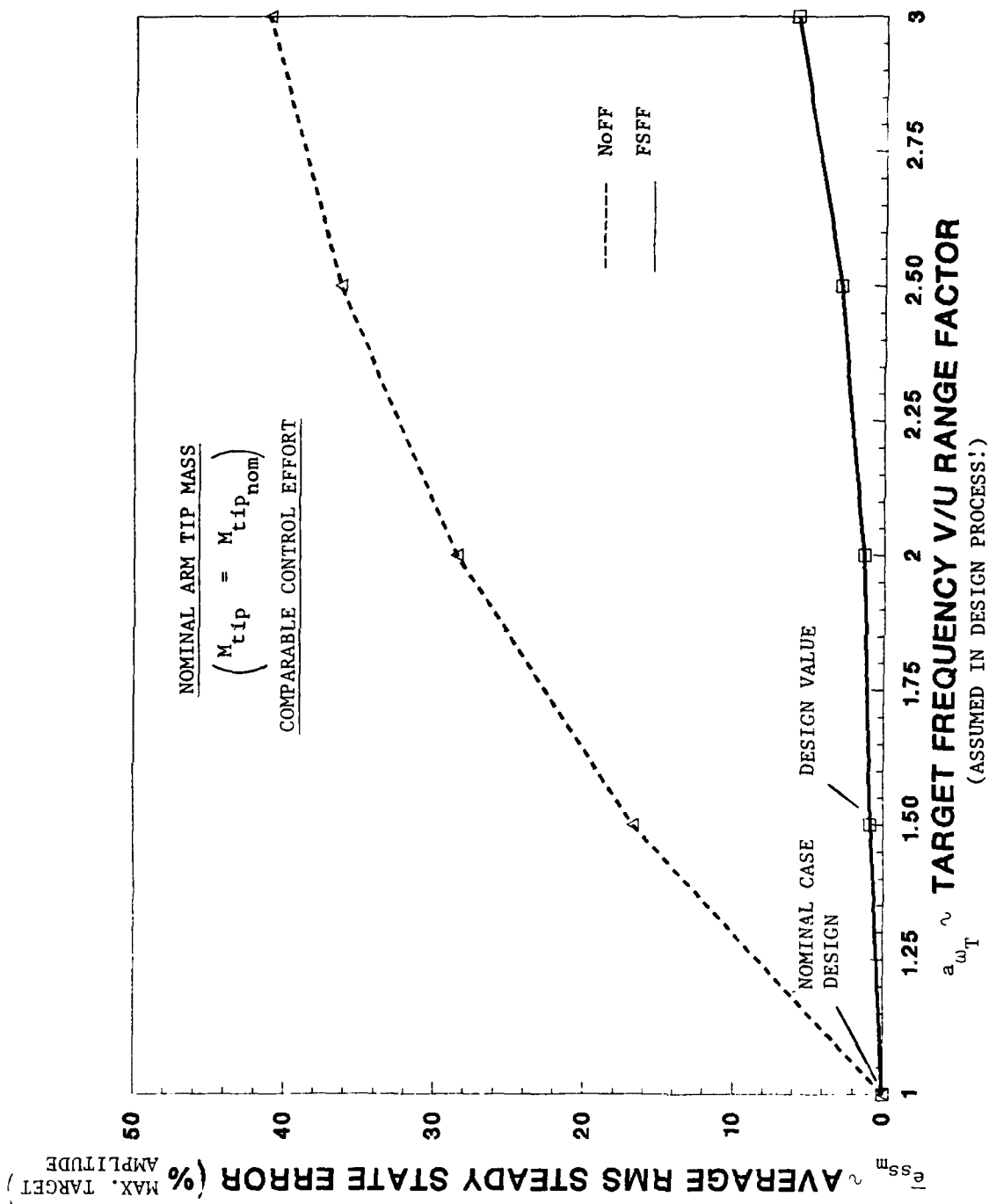


FIG. 12 EFFECT OF TARGET FREQUENCY VARIABILITY ON STEADY-STATE TRACKING: NoFF vs FSFF
 As target frequency variability/uncertainty range assumed in the design process increases, relative improvement in steady-state tracking accuracy obtained with feedforward also increases, confirming trends noted in Figs. (10)-(11)

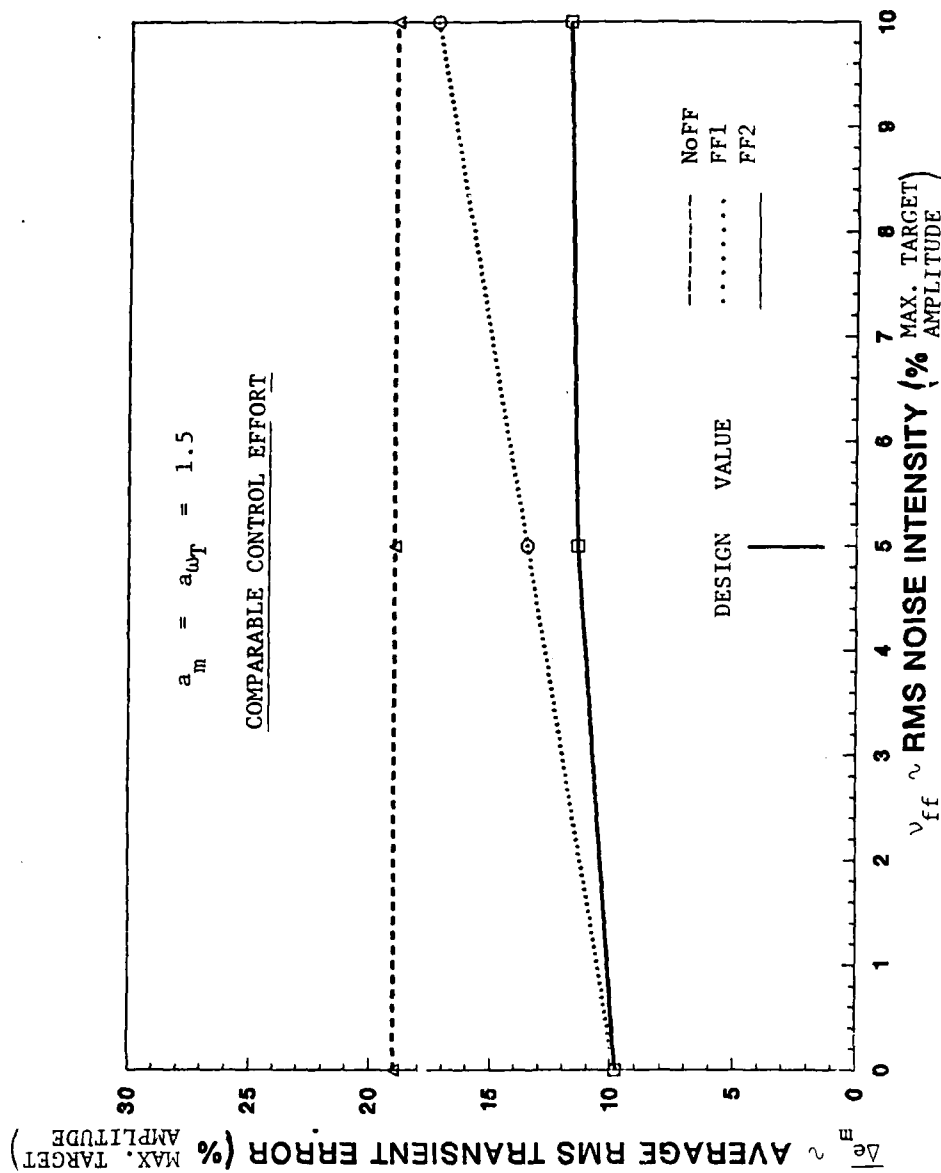


FIG. 13 EFFECT OF NOISE IN FEEDFORWARD MEASUREMENTS ON TRANSIENT TRACKING: NoFF vs FF1, FF2

Relative improvement in transient tracking performance afforded by feedforward of target position coordinates only (FF1) degrades rapidly as measurement noise increases. By eliminating the need to "differentiate" noisy target position measurements, feedforward of target rate measurements (FF2) recovers a significant amount of performance at higher design noise levels.

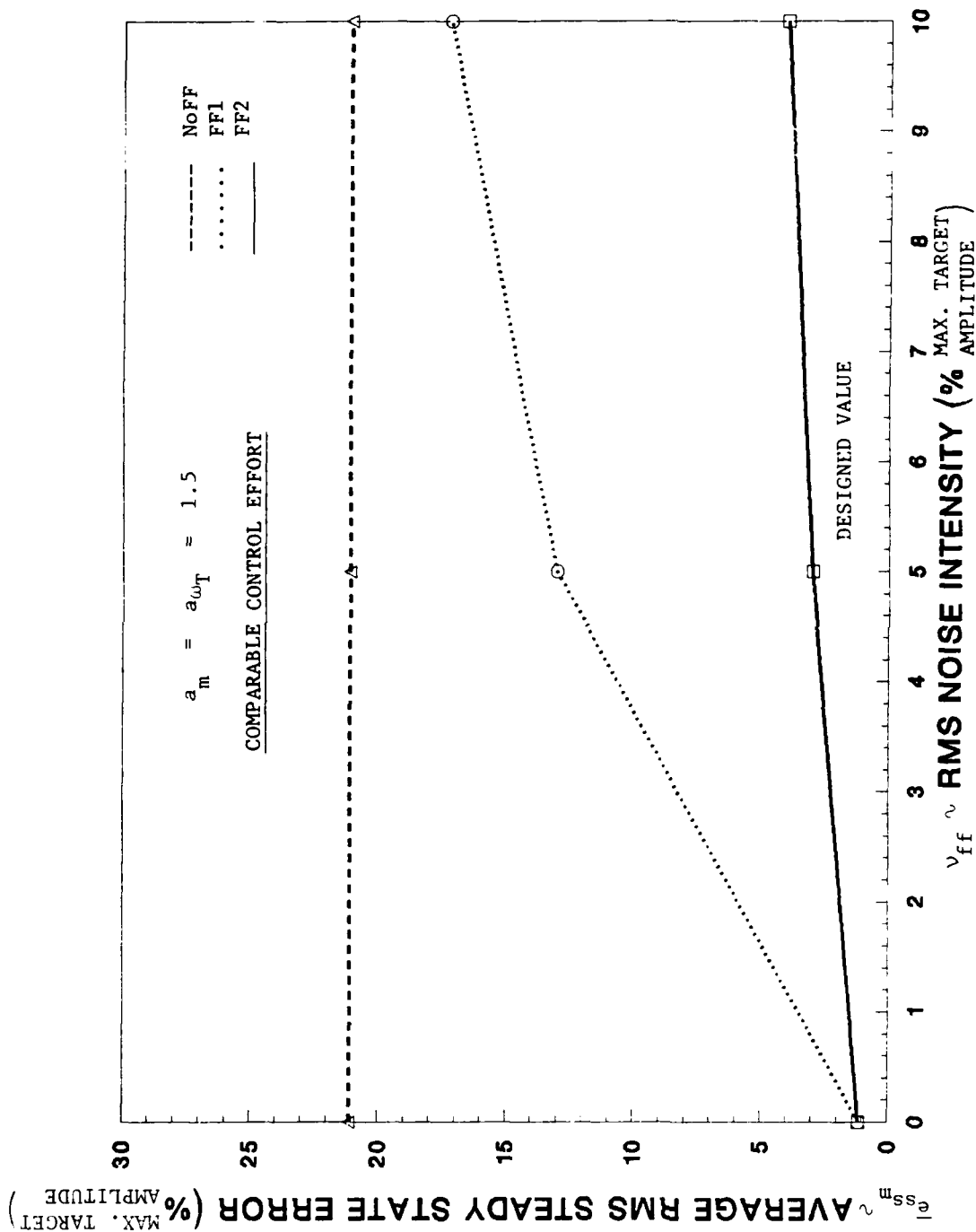


FIG. 14 EFFECT OF NOISE IN FEEDFORWARD MEASUREMENTS: "NoFF vs FF1, FF2"
 The trend observed in Fig. 13 is seen to hold for the comparative steady-state tracking performances: feedforward of target position and rate measurements significantly enhances steady-state tracking accuracy at higher design noise levels

TABLE 2
CLOSED LOOP DATA FOR OPTIMIZED 1L/1A CONTROLLERS DESIGNED
FOR FIVE PARAMETER CONDITIONS AND $\nu_{ff} = 5\%$

Controller Parameter Values	(I) NoFF	Controller (II)-a FF1	(III)-b FF2
K_e	106	106.8	47.2
K_{I_s}	-98.1	-7.24	30.3
K_{I_i}	46.3	.75	43.6
K_{I_r}	10.5	1.52	25.2
K_{θ}	-34.2	-13.39	-37.1
$I_s^* \equiv \begin{bmatrix} 0 & 1 \\ -a_2 & -a_1 \end{bmatrix}$	$\begin{bmatrix} 0 & 1 \\ -14.1 & -1.7 \end{bmatrix}$	$\begin{bmatrix} 0 & 1 \\ -18.3 & -.15 \end{bmatrix}$	$\begin{bmatrix} 0 & 1 \\ -21.1 & -2.3 \end{bmatrix}$
\hat{C}_{y_s}	-	-18.8	-13.7
\hat{C}_{v_s}	-	5.44	-.41
\hat{C}_{y_r}	-	0	9
\hat{C}_{v_r}	-	.0002	-.044
$[a_{T,1} \quad a_{T,2}]$	-	[-104.2 -10000]	[99 10000]
$[a_{T,1} \quad a_{T,2}]$	-	[-200.8 20000]	[34.7 20000]
$[b_{T,1} \quad b_{T,2}]$	-	-	[131.1 99.9]
$[b_{T,1} \quad b_{T,2}]$	-	-	[200.1 200]
Closed Loop Eigenvalues (Nominal Parameter) Condition	-2.04 \pm j6.17 -.042 \pm j.33 -24.9	-5.24 \pm j7.47 -.17 \pm j4.26 -.0147	-.84 \pm j6.77 -.48 \pm j.28 -29.25
Average Performance Data			
$\bar{\Delta}e_m$ (m)	.019	.014	.011
$\bar{e}_{ss,m}$ (m)	.021	.013	.003
$\Delta T_{c,m}^2$ (N-m) ²	3.96	3.65	4.48
$T_{c,m}^2$ (N-m) ²	56.2	40.9	75.3
$\bar{T}_{c,m}^2$ (N-m) ²	1.55	3.57	1.73

5.0 TWO-LINK, TWO-ACTUATOR MODEL

For this case, the nominal arm angles α and β at time $t = t_0^+$ are as shown in Fig. 2. Both torque motors A and B are assumed fully operative. It is desired to find control laws T_{c_A} and T_{c_B} that cause the arm (with variable M_{tip}) to track effectively a target undergoing elliptical motion at variable frequency ω_T superimposed on the rectilinear cable attachment point motion at constant velocity v_{R_0} . To account for variability/uncertainties in the eccentricity and orientation of the target elliptical motion, a random initial condition covariance matrix for the target motion was constructed and used in the design process as described below. The total distance $y_R(t_f)$ over which the target-tracking operation will occur is assumed small enough to allow for a linearized model of the arm angle perturbations from the nominal positions $\alpha_{nom} = 45^\circ$, $\beta_{nom} = -90^\circ$.

For design ranges of target frequency and arm tip mass variabilities (i.e. $a_{\omega_T} = a_m = 1.5$), and assuming white noise sources of equal power spectral density ($Q_{ff} = 2T\nu_{ff}^2$, where T is taken to be .005 secs and ν_{ff} is assumed to be 5% of the maximum expected target amplitude of .1 m) in each target state measurement, the NoFF and both ESFF controller structures are first designed and compared according to P.C. (A). Peak (continuous) allowable limits of 15 N-m (3 N-m) were assumed for each torque motor. The NoFF and FF1 structures are then redesigned according to P.C. (B) to determine the torque motor size required to match the tracking accuracy achieved with the FF2 controller.

5.1 Problem Formulation

Two-Link Arm Dynamics (linearized about α_{nom} , β_{nom}):

$$\begin{bmatrix} \dot{\alpha} \\ \ddot{\alpha} \\ \dot{\beta} \\ \ddot{\beta} \end{bmatrix} = \begin{bmatrix} 0 & 1 & 0 & 0 \\ 0 & 0 & 0 & 0 \\ 0 & 0 & 0 & 1 \\ 0 & 0 & 0 & 0 \end{bmatrix} \begin{bmatrix} \alpha \\ \dot{\alpha} \\ \beta \\ \dot{\beta} \end{bmatrix} + \begin{bmatrix} 0 & 0 \\ g_1^i & 0 \\ 0 & 0 \\ -g_1^i & g_2^i \end{bmatrix} \begin{bmatrix} T_{c_A} \\ T_{c_B} \end{bmatrix}; \quad X_o = \begin{bmatrix} 0 & 0 & 0 & 0 \\ 0 & 0 & 0 & 0 \\ 0 & 0 & 0 & 0 \\ 0 & 0 & 0 & 0 \end{bmatrix}$$

where g_1, g_2 depend on value of M_{tip} :

i	M_{tip}^i	g_1^i	g_2^i
1	.835	2.15	7.50
2	1.25	1.76	5.23
3	1.88	1.38	3.67

Target Dynamics:

$$\begin{bmatrix} \dot{x}_{T_r} \\ \ddot{x}_{T_r} \\ \dot{y}_{T_r} \\ \ddot{y}_{T_r} \\ \dot{y}_{T_r} \\ \ddot{y}_{T_r} \end{bmatrix} = \begin{bmatrix} 0 & 1 & 0 & 0 & 0 & 0 \\ -\omega_r^2 & 0 & 0 & 0 & 0 & 0 \\ 0 & 0 & 0 & 1 & 0 & 0 \\ 0 & 0 & -\omega_r^2 & 0 & 0 & 0 \\ 0 & 0 & 0 & 0 & 0 & 1 \\ 0 & 0 & 0 & 0 & 0 & 0 \end{bmatrix} \begin{bmatrix} x_{T_r} \\ \dot{x}_{T_r} \\ y_{T_r} \\ \dot{y}_{T_r} \\ y_{T_r} \\ \dot{y}_{T_r} \end{bmatrix};$$

$$X_{T_0}^i = \begin{bmatrix} .005 & 0 & 0 & 0 & \vdots & 0 & 0 \\ 0 & .005 \omega_r^{i^2} & 0 & 0 & \vdots & 0 & 0 \\ 0 & 0 & .005 & 0 & \vdots & 0 & 0 \\ 0 & 0 & 0 & .005 \omega_r^{i^2} & \vdots & 0 & 0 \\ \dots & \dots & \dots & \dots & \dots & \dots & \dots \\ 0 & 0 & 0 & 0 & \vdots & 0 & 0 \\ 0 & 0 & 0 & 0 & \vdots & 0 & .0004 \end{bmatrix}$$

Since we are unable to predict the eccentricity or orientation of the elliptical component of the target motion, the upper left quadrant of the target initial covariance matrix $X_{T_0}^i$ was chosen to be the same as for a *circular* trajectory of rms maximum radius .1m, random phase (this implies diagonal terms only), and frequency of traversal ω_r^i . The lower right quadrant precisely reflects the initial conditions associated with the ramp component of the target motion (i.e. $y_{T_r}(0) = 0; \dot{y}_{T_r}(0) = v_{R_0} = .02 \text{ m/sec}$).

Output Error Components:

$$e \equiv \begin{bmatrix} e_x \\ e_y \end{bmatrix}$$

$$e_x \equiv x_{T_s} - .3535 \alpha$$

$$e_y \equiv y_{T_s} + y_{T_r} - (.707 \alpha + .3535 \beta)$$

$$|e| \equiv \sqrt{e_x^2 + e_y^2}$$

Variable Parameters:

$$\frac{1}{1.5} \omega_{T_{nom}} \leq \omega_T^i \leq 1.5 \omega_{T_{nom}} \quad (\omega_{T_{nom}} = 2.84 \text{ rad/sec})$$

$$\frac{1}{1.5} M_{tip_{nom}} \leq M_{tip}^i \leq 1.5 M_{tip_{nom}} \quad (M_{tip_{nom}} = 1.253 \text{ kg})$$

5.2 Compensator Descriptions

(I) NoFF:

$$\begin{bmatrix} T_{c_A} \\ T_{c_B} \end{bmatrix} = \begin{bmatrix} T_{c_A}^* \\ T_{c_B}^* \end{bmatrix} = \begin{bmatrix} K_{e_{11}} & K_{e_{12}} \\ K_{e_{21}} & K_{e_{22}} \end{bmatrix} \begin{bmatrix} e_x \\ e_y \end{bmatrix} + \begin{bmatrix} K_{I_{s11}} & K_{I_{s12}} & K_{I_{s13}} & K_{I_{s14}} \\ K_{I_{s21}} & K_{I_{s22}} & K_{I_{s23}} & K_{I_{s24}} \end{bmatrix} \begin{bmatrix} z_{I_x} \\ \dot{z}_{I_x} \\ z_{I_y} \\ \dot{z}_{I_y} \end{bmatrix} \\ + \begin{bmatrix} K_{I_{r1}} \\ K_{I_{r2}} \end{bmatrix} z_{I_r} + \begin{bmatrix} K_{\dot{\alpha}_1} & K_{\dot{\alpha}_2} \\ K_{\dot{\beta}_1} & K_{\dot{\beta}_2} \end{bmatrix} \begin{bmatrix} \dot{\alpha} \\ \dot{\beta} \end{bmatrix}$$

where

$$\begin{bmatrix} \dot{z}_{I_{x_1}} \\ \ddot{z}_{I_{x_1}} \\ \dot{z}_{I_{y_1}} \\ \ddot{z}_{I_{y_1}} \end{bmatrix} = \begin{bmatrix} 0 & 1 & 0 & 0 \\ -a_{x_2} & -a_{x_1} & 0 & 0 \\ 0 & 0 & 0 & 1 \\ 0 & 0 & -a_{y_2} & -a_{y_1} \end{bmatrix} \begin{bmatrix} z_{I_{x_1}} \\ \dot{z}_{I_{x_1}} \\ z_{I_{y_1}} \\ \dot{z}_{I_{y_1}} \end{bmatrix} + \begin{bmatrix} 0 & 0 \\ a_{x_2} & 0 \\ 0 & 0 \\ 0 & a_{y_2} \end{bmatrix} \begin{bmatrix} e_x \\ e_y \end{bmatrix}$$

$$\dot{z}_{I_{y_1}} = e_y$$

Free Parameters for Optimization (22): $[K_c]; [K_{I_x}]; [K_{I_y}]; [K_{\dot{x}, \dot{y}}]; a_{x_1};$
 $a_{x_2}; a_{y_1}; a_{y_2}$

(II) ESFF (minimal realization forms):

$$\begin{bmatrix} T_{c_A} \\ T_{c_B} \end{bmatrix} = \begin{bmatrix} T_{c_A}^* \\ T_{c_B}^* \end{bmatrix} + \begin{bmatrix} \hat{C}_{11} & \hat{C}_{12} & \hat{C}_{13} & \hat{C}_{14} & \hat{C}_{15} & \hat{C}_{16} \\ \hat{C}_{21} & \hat{C}_{22} & \hat{C}_{23} & \hat{C}_{24} & \hat{C}_{25} & \hat{C}_{26} \end{bmatrix} \begin{bmatrix} \hat{z}_{x_{11}} \\ \hat{z}_{x_{12}} \\ \hat{z}_{y_{11}} \\ \hat{z}_{y_{12}} \\ \hat{z}_{y_{21}} \\ \hat{z}_{y_{22}} \end{bmatrix}$$

where, (FF1) (III)-a:

$$\begin{aligned}
 \text{(a)} \\
 \text{FF1:} \quad \begin{bmatrix} \dot{\hat{z}}_{x,1} \\ \dot{\hat{z}}_{x,2} \\ \dot{\hat{z}}_{y,1} \\ \dot{\hat{z}}_{y,2} \\ \dot{\hat{z}}_{y',1} \\ \dot{\hat{z}}_{y',2} \end{bmatrix} &= \begin{bmatrix} 0 & 1 & 0 & 0 & 0 & 0 \\ -a_{T_{x,2}} & -a_{T_{x,1}} & 0 & 0 & 0 & 0 \\ 0 & 0 & 0 & 1 & 0 & 0 \\ 0 & 0 & -a_{T_{y,2}} & -a_{T_{y,1}} & 0 & 0 \\ 0 & 0 & 0 & 0 & 0 & 1 \\ 0 & 0 & 0 & 0 & -a_{T_{y',2}} & -a_{T_{y',1}} \end{bmatrix} \begin{bmatrix} \hat{z}_{x,1} \\ \hat{z}_{x,2} \\ \hat{z}_{y,1} \\ \hat{z}_{y,2} \\ \hat{z}_{y',1} \\ \hat{z}_{y',2} \end{bmatrix} \\
 &+ \begin{bmatrix} 0 & 0 & 0 \\ a_{T_{x,2}} & 0 & 0 \\ 0 & 0 & 0 \\ 0 & a_{T_{y,2}} & 0 \\ 0 & 0 & 0 \\ 0 & 0 & a_{T_{y',2}} \end{bmatrix} \begin{bmatrix} z_1 \\ z_2 \\ z_3 \end{bmatrix}
 \end{aligned}$$

Free parameters for Optimization (40): Same as for NoFF plus: $[\hat{C}]$; $a_{T_{x,2}}$; $a_{T_{x,1}}$; $a_{T_{y,1}}$; $a_{T_{y,2}}$; $a_{T_{y',1}}$; $a_{T_{y',2}}$

$$\begin{aligned}
 \text{(b)} \\
 \text{FF2:} \quad \begin{bmatrix} \dot{\hat{z}}_{x,1} \\ \dot{\hat{z}}_{x,2} \\ \dot{\hat{z}}_{y,1} \\ \dot{\hat{z}}_{y,2} \\ \dot{\hat{z}}_{y',1} \\ \dot{\hat{z}}_{y',2} \end{bmatrix} &= \begin{bmatrix} 0 & 1 & 0 & 0 & 0 & 0 \\ -a_{T_{x,2}} & -a_{T_{x,1}} & 0 & 0 & 0 & 0 \\ 0 & 0 & 0 & 1 & 0 & 0 \\ 0 & 0 & -a_{T_{y,2}} & -a_{T_{y,1}} & 0 & 0 \\ 0 & 0 & 0 & 0 & 0 & 1 \\ 0 & 0 & 0 & 0 & -a_{T_{y',2}} & -a_{T_{y',1}} \end{bmatrix} \begin{bmatrix} \hat{z}_{x,1} \\ \hat{z}_{x,2} \\ \hat{z}_{y,1} \\ \hat{z}_{y,2} \\ \hat{z}_{y',1} \\ \hat{z}_{y',2} \end{bmatrix} \\
 &+ \begin{bmatrix} 0 & b_{T_{x,1}} & 0 & 0 & 0 & 0 \\ a_{T_{x,2}} & b_{T_{x,2}} & 0 & 0 & 0 & 0 \\ 0 & 0 & 0 & b_{T_{y,1}} & 0 & 0 \\ 0 & 0 & a_{T_{y,2}} & b_{T_{y,2}} & 0 & 0 \\ 0 & 0 & 0 & 0 & 0 & b_{T_{y',1}} \\ 0 & 0 & 0 & 0 & a_{T_{y',2}} & b_{T_{y',2}} \end{bmatrix} \begin{bmatrix} z_1 \\ z_2 \\ z_3 \\ z_4 \\ z_5 \\ z_6 \end{bmatrix}
 \end{aligned}$$

Free Parameters for Optimization (46): Same as for FF1 plus: $b_{T_{x,1}}$; $b_{T_{x,2}}$; $b_{T_{y,1}}$;
 $b_{T_{y,2}}$; $b_{T_{v,1}}$; $b_{T_{v,2}}$

where,

$$z_1 = x_{T_e} + \nu_1$$

$$z_2 = x_{T_e} + \nu_2$$

$$z_3 = y_{T_e} + \nu_3$$

$$z_4 = y_{T_e} + \nu_4$$

$$z_5 = y_{T_e} + \nu_5$$

$$z_6 = y_{T_e} + \nu_6$$

Each noise input ν_i is assumed to be exponentially correlated with rms intensity $\nu_{ff} = 5\%$ of maximum expected target amplitude (.1m) and correlation time $T = .005\text{secs}$. Since this represents a relatively short interval compared with anticipated correlation times for the target motion, for analytic convenience we shall model each ν_i as a white noise source with power spectral density Q_{ff} as follows:

$$E(\nu_i(t)\nu_j(\tau)) = Q_{ff} \delta_{ij} (t - \tau)$$

$$Q_{ff} = 2T\nu_{ff}^2 = .01\nu_{ff}^2 = .25 \times 10^{-6} \text{m}^2\text{-sec}$$

5.3 Controller Design and Performance Criteria for 2L/2A Arm

P.C. (A): For

$$\max (|T_{eA}^i(t)|, |T_{eB}^i(t)|) \leq 15 \text{ N-m} \quad (i = 1, np; t = t_0, t_f)$$

$$\max (\overline{T_{eA,ssm}}, \overline{T_{eB,ssm}}) \leq 3 \text{ N-m}$$

minimize a weighted sum of mean square transient and steady-state tracking errors averaged over the np parameter conditions:

$$\overline{e^{2^*}} \equiv \frac{\sum_{i=1}^{np} e^{2^*i}}{np}; \quad e^{2^*i} \equiv q_{ss} e_{ss,m}^{i'} e_{ss,m}^i + q \Delta e_m^{i'} \Delta e_m^i$$

P.C. (B): For

$$\Delta e_m^{i'} \Delta e_m^i dt \leq N_{\Delta}$$

$$e_{ss,m}^{i'} e_{ss,m}^i \leq N_{ss}$$

where N_{Δ} and N_{ss} are to be chosen based on results using P.C. (A), minimize a weighted sum of peak and steady-state torques averaged over the np parameter conditions (as for the 1L/1A case we use the first two terms below as a quadratic surrogate for peak torque):

$$\overline{T_c^{2^*}} \equiv \frac{\sum_{i=1}^{np} T_c^{2^*i}}{np}; \quad T_c^{2^*i} \equiv r_o T_{c_{om}}^{i'} T_{c_{om}}^i + r \Delta T_{c_m}^{i'} \Delta T_{c_m}^i + r_{ss} T_{c_{ss,m}}^{i'} T_{c_{ss,m}}^i$$

For either performance criterion, define a quadratic cost function:

$$J^* \equiv \sum_{i=1}^{np} \rho^i J^i$$

$$J^i \equiv q_{ss} e_{ss,m}^{i'} e_{ss,m}^i + q \Delta e_m^{i'} \Delta e_m^i + r_o T_{c_{om}}^{i'} T_{c_{om}}^i + r \Delta T_{c_m}^{i'} \Delta T_{c_m}^i + r_{ss} T_{c_{ss,m}}^{i'} T_{c_{ss,m}}^i$$

When carrying out the design according to P.C. (A), weighting parameters q_{ss} and q are first chosen (on a trial and error basis for each structure) to provide a good balance between steady-state and transient tracking accuracy. For this choice, r , r_o , r_{ss} are then varied iteratively by the designer until the corresponding solution for minimization of J^* yields:

$$(i) \max \{ \overline{\Delta T_{c_{Am}}^2}, \overline{\Delta T_{c_{Bm}}^2} \} \leq 4 \text{ (N-m)}^2$$

$$(ii) \max \{ \overline{T_{c_{Aom}}^2}, \overline{T_{c_{Bom}}^2} \} \leq 100 \text{ (N-m)}^2$$

$$(iii) \max \{ \overline{T_{c_{Assm}}^2}, \overline{T_{c_{Bssm}}^2} \} \leq 4 \text{ (N-m)}^2$$

where, to ensure uniqueness of the solution, we further require that each control term weighting parameter be zero unless the corresponding constraint (i), (ii), or (iii) is active (i.e. the equality relation holds).

Conversely, for P.C. (B), we shall set r , r_0 , r_{ss} at fixed values (based on results for FF2 using P.C. (A)) and vary q_{ss} , q until the optimal solution yields:

$$\overline{e'_{ssm} e_{ssm}} \leq N_{ss}$$

N_{ss} , N_{Δ} set to corresponding values
of FF2 controller designed for P.C. (A).

$$\overline{\Delta e'_m \Delta e_m} \leq N_{\Delta}$$

6.0 DESIGN RESULTS FOR 2L/2A MODEL ($a_{\omega_T} = a_M = 1.5$, $\nu_{ff} = 5\%$)

Five discrete parameter conditions (identical to those for the 1L/1A case) were used to bracket the design parameter variability ranges. Tables (3) and (4) summarize average closed loop performance data for the controller structures optimized according to P.C. (A). For specified bounds on control effort, it is apparent that the comparative abilities of the three controllers to minimize steady-state and transient tracking errors follows the same trend as observed for the 1L/1A case. Feedforward of target position and velocity coordinates (FF2) is seen to offer a 44% reduction in average root mean square transient tracking error $\overline{\Delta e_m}$ and a large improvement (88% reduction) in average root mean square steady-state error $\overline{e_{ssm}}$. Feedforward of only target position coordinates (FF1) provides less dramatic improvements (23% reduction in $\overline{\Delta e_m}$, 32% reduction in $\overline{e_{ssm}}$).

Figures 15 and 16 exemplify robustness characteristics associated with the optimized controllers. For the heavy tip mass (i.e. "worst") case, sensitivities of average root mean square transient and steady-state tracking errors to actual target frequency variations are shown. Note that, over the entire design range of ω_T variability, the optimized FF2 controller in particular provides significantly improved tracking accuracy relative to the NoFF controller given the same constraints on control effort.

It is important at this point to analyze the final designs in more detail to check whether the original design goals stated in Section 2.0 have been satisfied. To reiterate these goals:

- (1) error settling time to 1 cm (i.e. 10% of average expected target amplitude) ≤ 10 secs
- (2) peak torque ≤ 15 N-m
- (3) rms continuous (steady-state) torque ≤ 3 N-m

To check precisely whether each of the goals have been met for every possible combination of arm/target parameters and initial conditions would require an infinite number of analytic evaluations and/or simulation runs. For the purposes of this design study, we shall check by simulation only the five design points used to bracket the parameter variability ranges and assume a "worst-case" set of initial conditions.¹ The results of this evaluation are contained in Table (5). It is seen that the FF2 controller is by far the most consistent in achieving the 10 second settling time goal except at v/u parameter condition 3, at which 12.4 seconds is required for settling to the 10% goal. This condition corresponds to the case where M_{tip} and ω_r are 50% higher than their respective nominal values, and would intuitively seem to be the most difficult condition for which to provide good control. Neither FF1 nor NoFF achieved the 10% goal before 10 seconds at any of the v/u parameter conditions checked. In fact, with the exception of the FF1 controller at the nominal parameter condition (1), the tracking errors associated with FF1 and NoFF are observed *never* to settle below 10%. In terms of peak control torque encountered, all three controllers are seen to meet the design constraint of 15 N-m, with T_{c_B} of the NoFF controller coming the closest to violation with a 14.7 N-m excursion which occurred at $t = 0^+$ in response to the assumed worst case initial error of .1265 m. Rms continuous torques are also seen to lie safely below the allowable limit of 3 N-m.

Discrete-time linear simulations for the three controller structures optimized to P.C. (A), including the effects of feedforward measurement noise, are shown in Figs. 17-20. The first two figures present comparative time histories for the position error magnitude and the two control torques T_{c_A} and T_{c_B} for the case of nominal arm tip mass/target frequency and worst-case initial conditions. Feedforward measurement noise roughly equivalent to that assumed in the design ($\nu_{ff} = 5\%$) was simulated using a random number generating routine. The FF2 controller clearly meets the design goals of Section 2.0 at this particular condition: the position error magnitude is seen to settle to the 10% goal after only 3 secs compared with the required settling time of 10 secs. By contrast, the FF1 controller is seen to require a 16 sec settling time while the NoFF controller never settles below 10%. The control torque histories for this condition are quite similar for all controllers, as expected (due to identical control torque constraints

¹ i.e. the case where $x_o = [0]$ and $x_{r_o} = [.1265, 0, 0, -.1795, 0, .02]'$ which corresponds to target elliptical motion with average amplitude = .1 m and eccentricity = .866.

assumed in the design process). The peak torque constraint of ± 15 N-m is met by all three controllers at this condition. Note the greater noise response associated with the control torque histories of the FF1 controller using noisy target position measurements only. Figures 19-20 show comparative time histories for the (worst) case parameter condition where the arm tip mass and target frequency are each 50% higher than their nominal values. In this case, the position error magnitude for the FF2 controller is seen to require slightly greater than 4 secs to settle below the 10% goal, while the NoFF controller and the FF1 controller never settle below 10% for the same constraints on control effort.

The above results indicate that the FF2 controller requiring sensors for both target position and rate coordinates should be implemented in order to meet design goals for tracking accuracy without violating the given control constraints. It is of interest to know how much larger the torque motor limits would have to be for the NoFF and FF1 controllers (requiring fewer sensors) to match the tracking accuracy achieved with FF2. Accordingly, both the NoFF and the FF1 structures were re-optimized using P.C. (B) of Section 5.0, with numerical bounds N_{Δ} and N_{ω} on the average root mean square transient and steady-state errors assumed to be the corresponding values associated with the FF2 controller optimized using P.C.(A) (which appears to very nearly satisfy all design goals). Results of this re-optimization indicated that the torque motor peak limits would have to be approximately (40 N-m) and (20 N-m) to accomodate error requirements with NoFF and FF1, respectively. Thus, if torque motor size were a variable in the overall system design process, the designer would have to weigh the costs of obtaining larger torque motors and using fewer sensors against using smaller torque motors and more sensors.

TABLE 3
CLOSED LOOP CONTROLLER PARAMETERS FOR OPTIMIZED 2L/2A CONTROLLERS
DESIGNED FOR FIVE PARAMETER CONDITIONS AND $\gamma_{ff} = 5\%$

Controller Parameter Values	(I) NoFF	(III)-a FFI	(II)-b FF2
$[K_e]$	$\begin{bmatrix} -55.5 & 70.6 \\ 115.1 & 80.4 \end{bmatrix}$	$\begin{bmatrix} -58.3 & 71.1 \\ 98.4 & 76.9 \end{bmatrix}$	$\begin{bmatrix} -66.4 & 79.0 \\ 96.2 & 67.2 \end{bmatrix}$
$[K_{Is}]$	$\begin{bmatrix} 94.6 & -26.3 & -59.8 & 41.8 \\ -62.1 & 86.9 & -45.3 & 104.7 \end{bmatrix}$	$\begin{bmatrix} 84.9 & -20.7 & -55.1 & 41.2 \\ -53.2 & 85.0 & -47.2 & 103 \end{bmatrix}$	$\begin{bmatrix} 75.6 & -33.7 & -41.8 & 62.9 \\ -55.5 & 84.1 & -44.3 & 99.4 \end{bmatrix}$
$[K_{Ir}]$	$\begin{bmatrix} 12.04 \\ 15.70 \end{bmatrix}$	$\begin{bmatrix} 12.89 \\ 19.94 \end{bmatrix}$	$\begin{bmatrix} 35.3 \\ 25.8 \end{bmatrix}$
$[K_{\alpha, \beta}]$	$\begin{bmatrix} -15.04 & -1.87 \\ -20.0 & -20.6 \end{bmatrix}$	$\begin{bmatrix} 8.87 & -1.59 \\ -13.67 & -10.61 \end{bmatrix}$	$\begin{bmatrix} -15.1 & -1.67 \\ -13.8 & -12.7 \end{bmatrix}$
$I_s^* = \begin{bmatrix} 0 & 1 & 0 & 0 \\ -ax_2 & -ax_1 & 0 & 0 \\ 0 & 0 & 1 & 0 \\ 0 & 0 & -ay_2 & -ay_1 \end{bmatrix}$	$\begin{bmatrix} 0 & 0 & 0 & 0 \\ -13.3 & -1.16 & 0 & 0 \\ 0 & 0 & 0 & 0 \\ 0 & 0 & -13.1 & -1.38 \end{bmatrix}$	$\begin{bmatrix} 0 & 1 & 0 & 0 \\ -7.5 & -1.12 & 0 & 0 \\ 0 & 0 & 0 & 1 \\ 0 & 0 & -10.9 & -1.43 \end{bmatrix}$	$\begin{bmatrix} 0 & 1 & 0 & 0 \\ -13.1 & -2.2 & 0 & 0 \\ 0 & 0 & 0 & 1 \\ 0 & 0 & -11.1 & -2.6 \end{bmatrix}$
$[C]$	$\begin{bmatrix} 19.2 & -3.7 & -16.1 & 1.2 & 0 & -.06 \\ -18.1 & 1.2 & -10.6 & .34 & 0 & .02 \end{bmatrix}$	$\begin{bmatrix} 19.2 & -3.7 & -16.1 & 1.2 & 0 & -.06 \\ -18.1 & 1.2 & -10.6 & .34 & 0 & .02 \end{bmatrix}$	$\begin{bmatrix} 8.8 & .24 & -8.04 & -.15 & 0 & -.09 \\ -5.2 & -.2 & -5.7 & -.12 & 0 & -.08 \end{bmatrix}$
$\begin{bmatrix} a_{Txs1} & a_{Txs2} & \dots & a_{Ty1} & a_{Ty2} \end{bmatrix}$	$\begin{bmatrix} -10000 \\ -106.1 \\ -20000 \\ -106.2 \\ -30000 \\ -100.6 \end{bmatrix}$	$\begin{bmatrix} -10000 \\ -106.1 \\ -20000 \\ -106.2 \\ -30000 \\ -100.6 \end{bmatrix}$	$\begin{bmatrix} -10000 \\ -96.3 \\ 20000 \\ -96.9 \\ -30000 \\ -100.3 \end{bmatrix}$
$\begin{bmatrix} b_{Txs1} & b_{Txs2} & \dots & b_{Ty1} & b_{Ty2} \end{bmatrix}$	$\begin{bmatrix} 0 \\ 10000 \\ 0 \\ 20000 \\ 0 \\ 30000 \end{bmatrix}$	$\begin{bmatrix} 0 \\ 10000 \\ 0 \\ 20000 \\ 0 \\ 30000 \end{bmatrix}$	$\begin{bmatrix} 109.2 \\ 100.0 \\ 200.1 \\ 200.0 \\ 300.2 \\ 300.0 \end{bmatrix}$

TABLE 4
AVERAGE PERFORMANCE DATA FOR OPTIMIZED 2L/2A CONTROLLERS
DESIGNED FOR FIVE PARAMETER CONDITIONS AND $\nu_{ff} = 5\%$

Average Performance Values	Controller		
	(I) NoFF	(II)-a FF1	(III)-b FF2
$\overline{\Delta T}_{c_{Am}}^2 \text{ (N-m)}^2$	3.6	3.91	4.05
$\overline{\Delta T}_{c_{Bm}}^2 \text{ (N-m)}^2$	2.27	2.88	2.84
$\overline{T}_{c_{Aom}}^2 \text{ (N-m)}^2$	40.3	23.8	81.7
$\overline{T}_{c_{Bom}}^2 \text{ (N-m)}^2$	99.3	54.4	95.6
$\overline{T}_{c_{Assm}}^2 \text{ (N-m)}^2$	1.2	3.41	1.26
$\overline{T}_{c_{Bssm}}^2 \text{ (N-m)}^2$.376	.59	.39
$\overline{\Delta e_m} \text{ (m)}$.0236	.0181	.0133
$\overline{e_{ssm}} \text{ (m)}$.0205	.014	.0025
Closed Loop Eigenvalues (Nominal Parameter) Condition	-72.6	-33.9	-41.7
	-21.5	-7.7	-20.4
	$-1.91 \pm j7.6$	$-2.95 \pm j8.8$	$-2.66 \pm j9.1$
	$-1.94 \pm j6.6$	$-2.28 \pm j7.9$	$-2.31 \pm j7.15$
	$-.04 \pm j.29$	$-.08 \pm j.40$	$-.13 \pm j.54$
	-.016	-.034	-.201

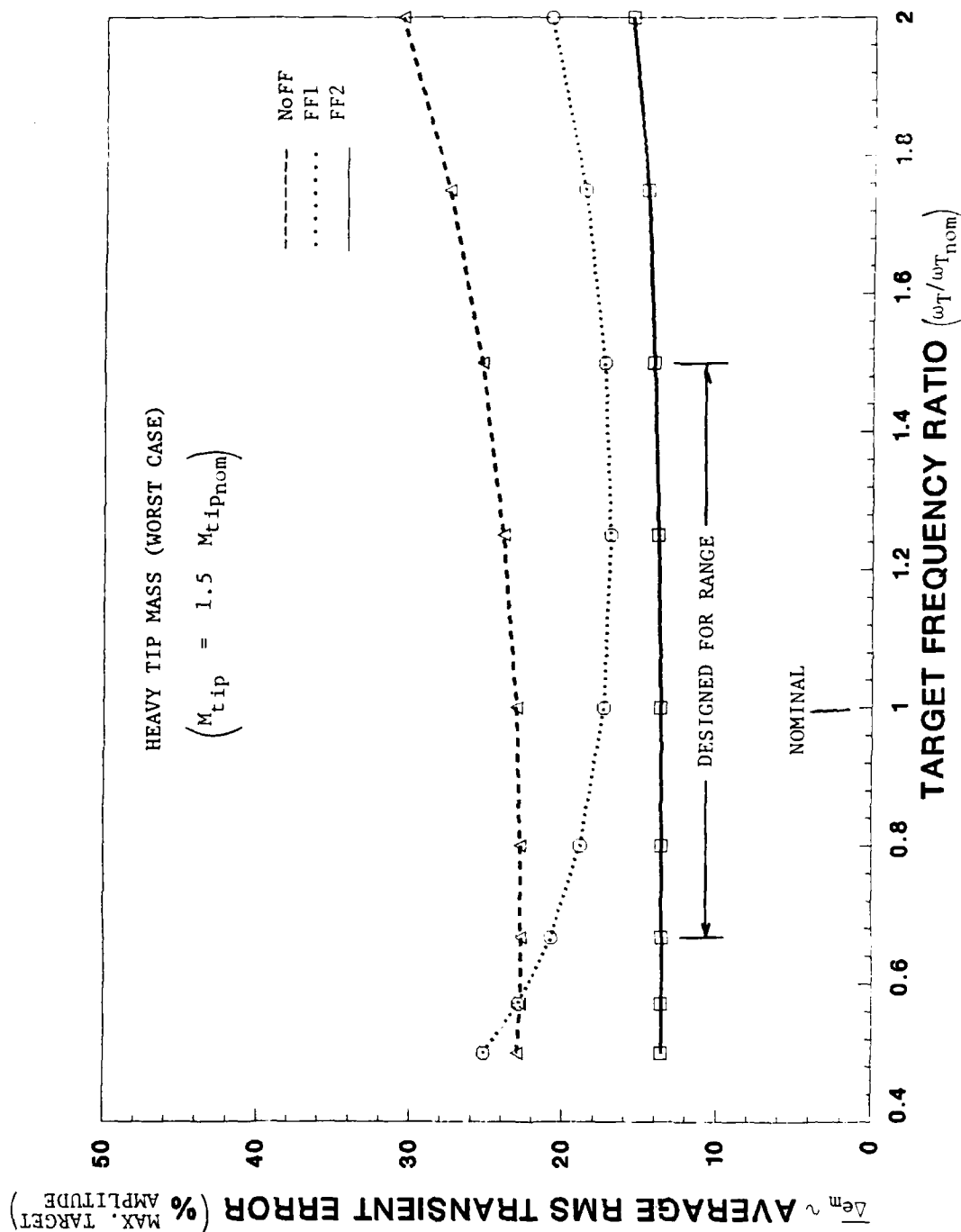


FIG. 15 ROBUSTNESS OF TRANSIENT TRACKING RESPONSE TO ACTUAL VARIATIONS IN TARGET FREQUENCY
 Over the entire "designed-for range" of target frequencies, feedforward of target position and rate coordinates (FF2) produces the lowest transient tracking errors for comparable levels of control effort

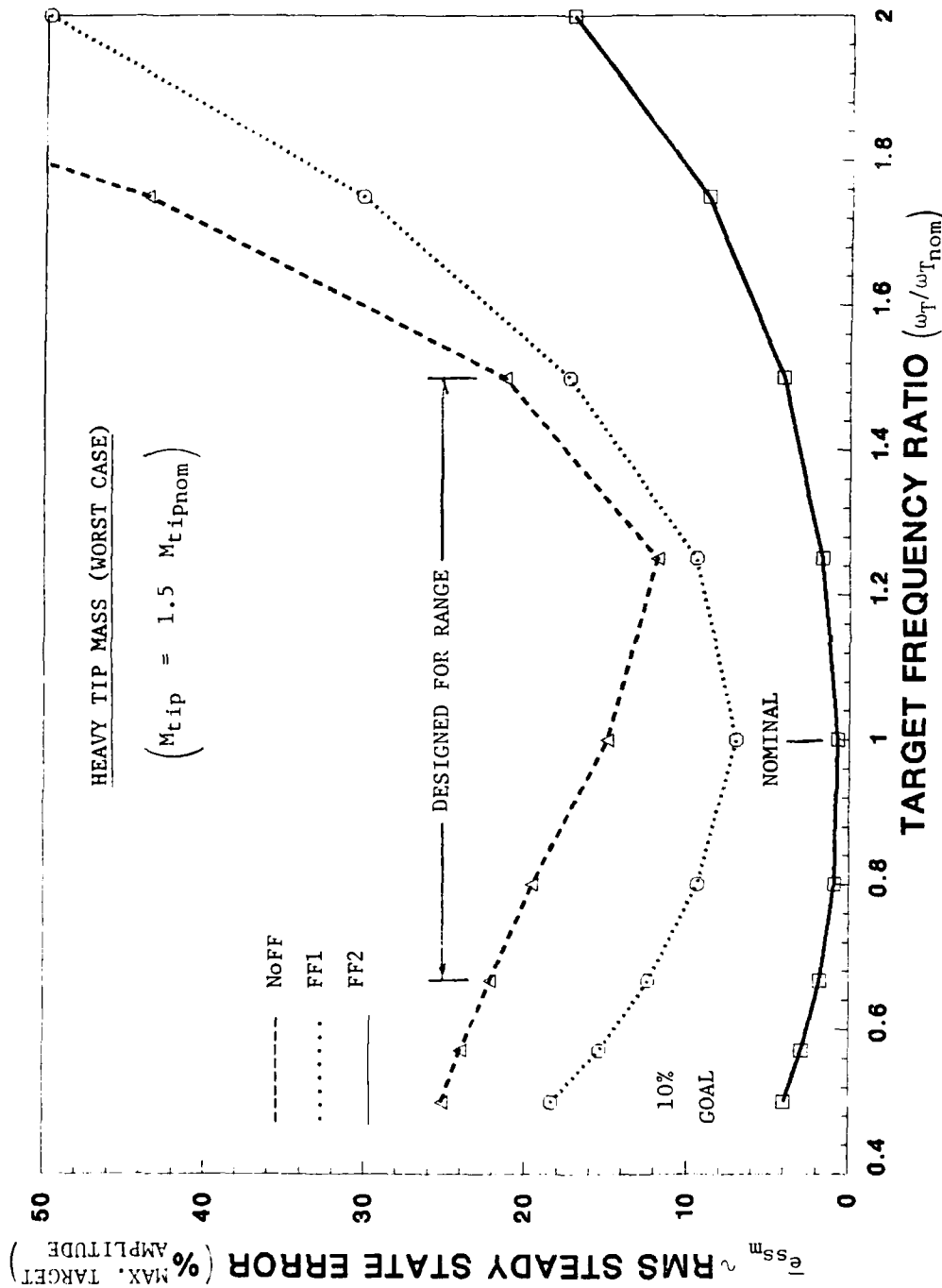


FIG. 16 ROBUSTNESS OF STEADY-STATE TRACKING RESPONSE TO ACTUAL VARIATIONS IN TARGET FREQUENCY
 Feedforward of target position and rate coordinates (FF2) is required if the 10% goal
 is to be realized over the entire "designed-for range" for given constraints on the
 control effort

TABLE 5
COMPARATIVE CONTROLLER PERFORMANCE AT WORST CASE INITIAL CONDITIONS VS. DESIGN GOALS

Performance Criterion	NoFF					FF1					FF2				
	v/u Param. Cond. No.					v/u Param. Cond. No.					v/u Param. Cond. No.				
	1	2	3	4	5	1	2	3	4	5	1	2	3	4	5
I. Error Settling Time to 'X' % of Average Target Position Amplitude (= 10 cm) <u>X (%)</u>	(Goal ≤ 10 secs) to 10%					(Goal ≤ 10 secs) to 10%					(Goal ≤ 10 secs) to 10%				
	Set. Time* (secs)					Set. Time* (secs)					Set. Time* (secs)				
	8	9	-	-	-	.4	1	1	1	1	.9	1	1	1	1
	25	-	-	-	-	.42	14.2	15.8	14.2	14.2	1.0	1.3	1.1	1.3	1.1
	20	-	-	-	-	.9	-	-	-	-	2.2	1.9	2.6	1.8	2.6
	15	-	-	-	-	16	-	-	-	-	3.0	3.9	4.1	4.1	3.9
	10	-	-	-	-	-	-	-	-	-	8.0	11.2	-	14.3	12.8
	5	-	-	-	-	-	-	-	-	-	-	-	-	-	-
II. Maximum Control Torques (N-m) $ T_{cA}(t) _{\max}$ $ T_{cB}(t) _{\max}$	(Goal ≤ 15 N-m)					(Goal ≤ 15 N-m)					(Goal ≤ 15 N-m)				
	7.2	7.2	7.2	7.2	7.2	6.1	6.1	6.1	6.1	6.1	10.5	9.4	12.2	9.4	12.3
	14.7	14.7	14.7	14.7	14.7	10.5	10.5	10.5	10.5	10.5	8.7	9.5	7.5	9.6	7.5
III. RMS Continuous Control Torques (N-m) $T_{cA_{SSM}}$ $T_{cB_{SSM}}$	(Goal ≤ 3 N-m)					(Goal ≤ 3 N-m)					(Goal ≤ 3 N-m)				
	.54	.27	2.0	.18	1.25	1.6	1.5	2.46	1.52	1.92	.7	.45	1.98	.35	1.25
	.28	.18	1.2	.08	.52	.56	.52	1.30	.46	.68	.4	.32	1.17	.23	.53

*Note: A dash (i.e. '-') indicates "never settles to v %".

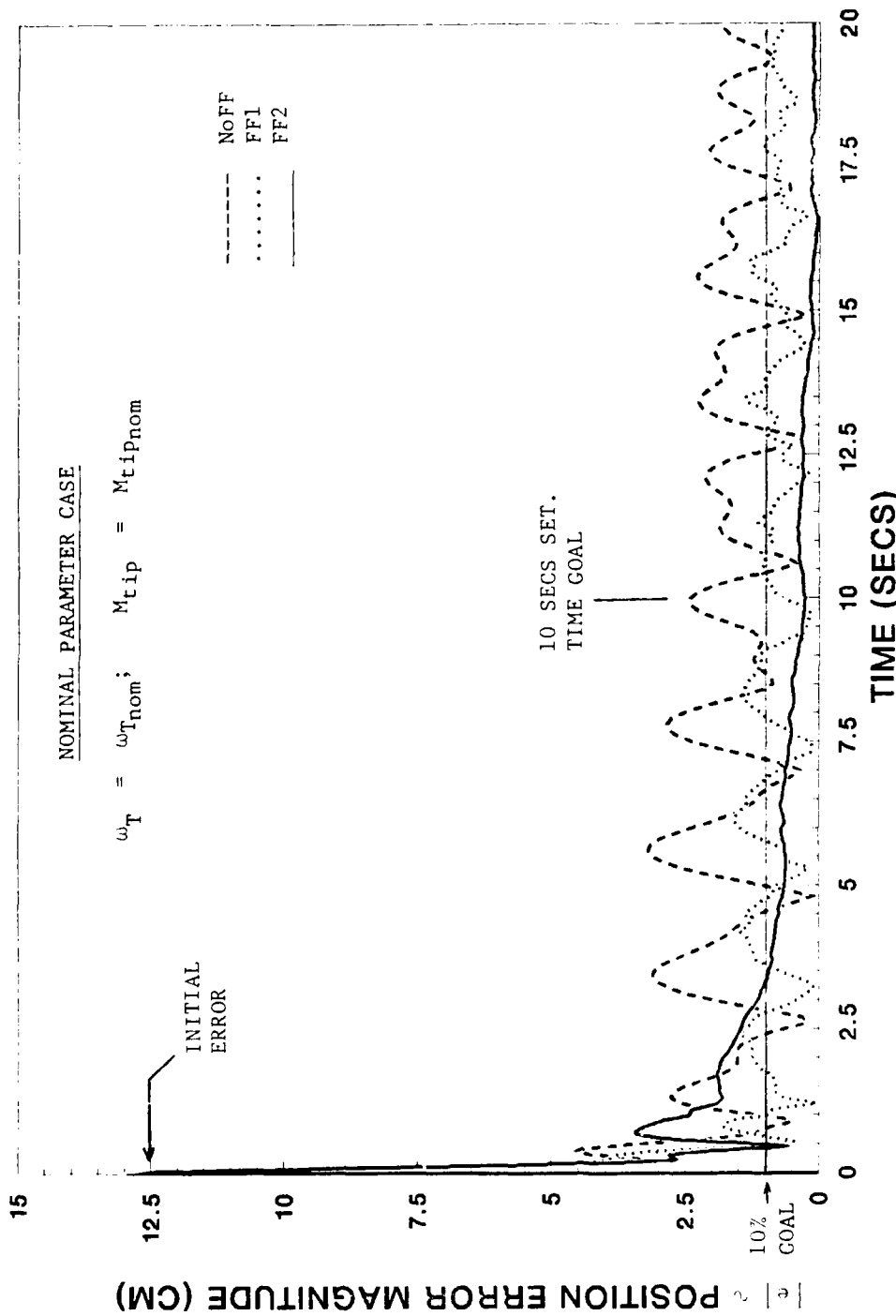


FIG. 17 POSITION ERROR MAGNITUDE HISTORIES OF TRACKING CONTROLLERS NOMINAL PARAMETERS CASE

By feeding forward target position and rate coordinates (FF2) settling time and steady state accuracy goals are easily met. Feedforward of target position coordinates only (FF1) offers some improvement relative to NoFF, but not quite enough to meet objectives

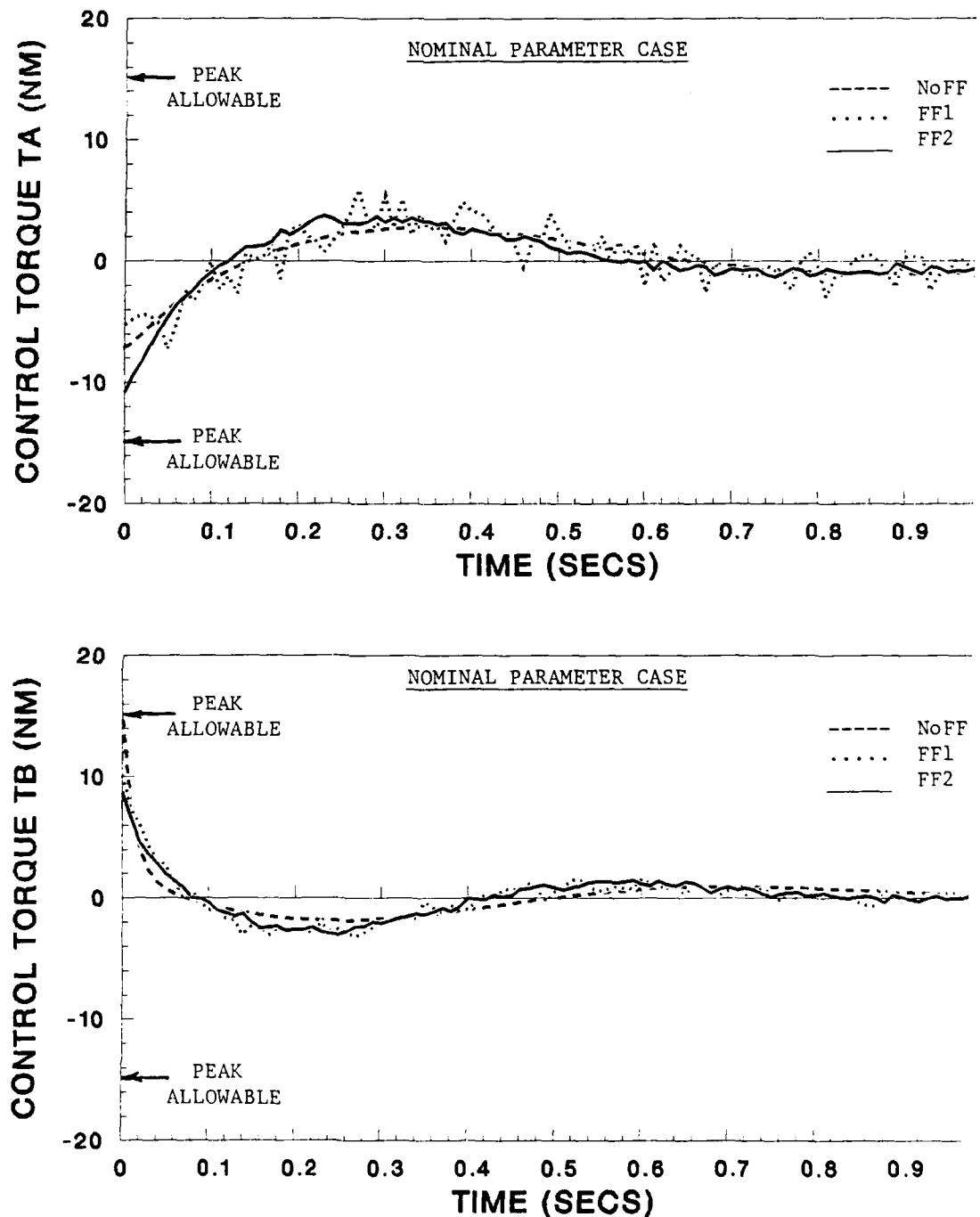


FIG. 18 CONTROL TORQUE HISTORIES OF TRACKING CONTROLLERS NOMINAL PARAMETERS
Control torque histories producing tracking error responses of Fig. 17. All three controllers exhibit comparable control effort. Peak and continuous constraints are satisfied in each case

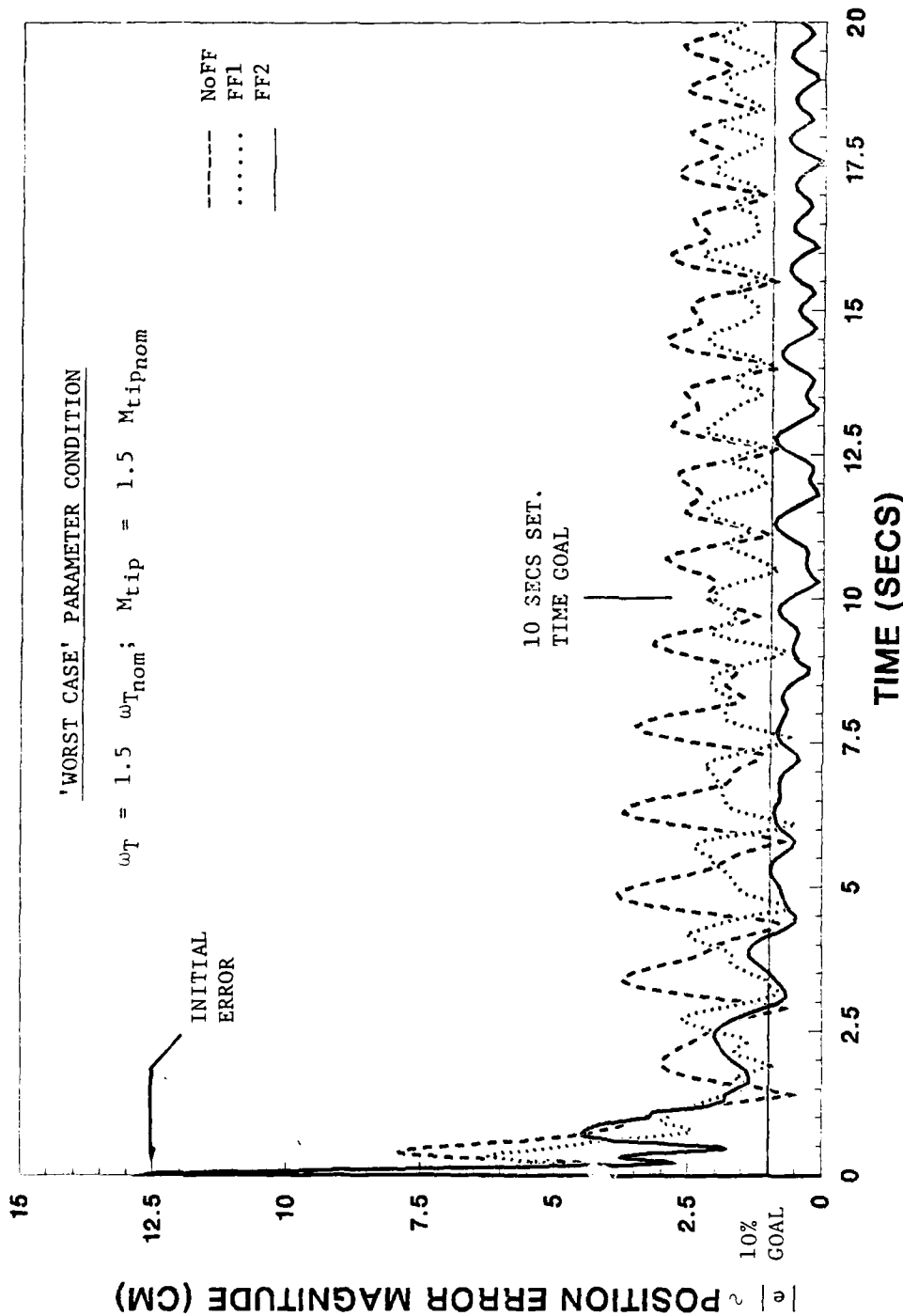


FIG. 19 POSITION ERROR MAGNITUDE HISTORIES OF TRACKING CONTROLLERS WORST PARAMETERS CASE

Even at the worst case parameter condition, feedforward of target position and rate coordinates (FF2) satisfies settling time and steady state accuracy goals. Without feedforward (NoFF) or with feedforward of target position coordinates only (FF1), the tracking control clearly fails to meet objectives

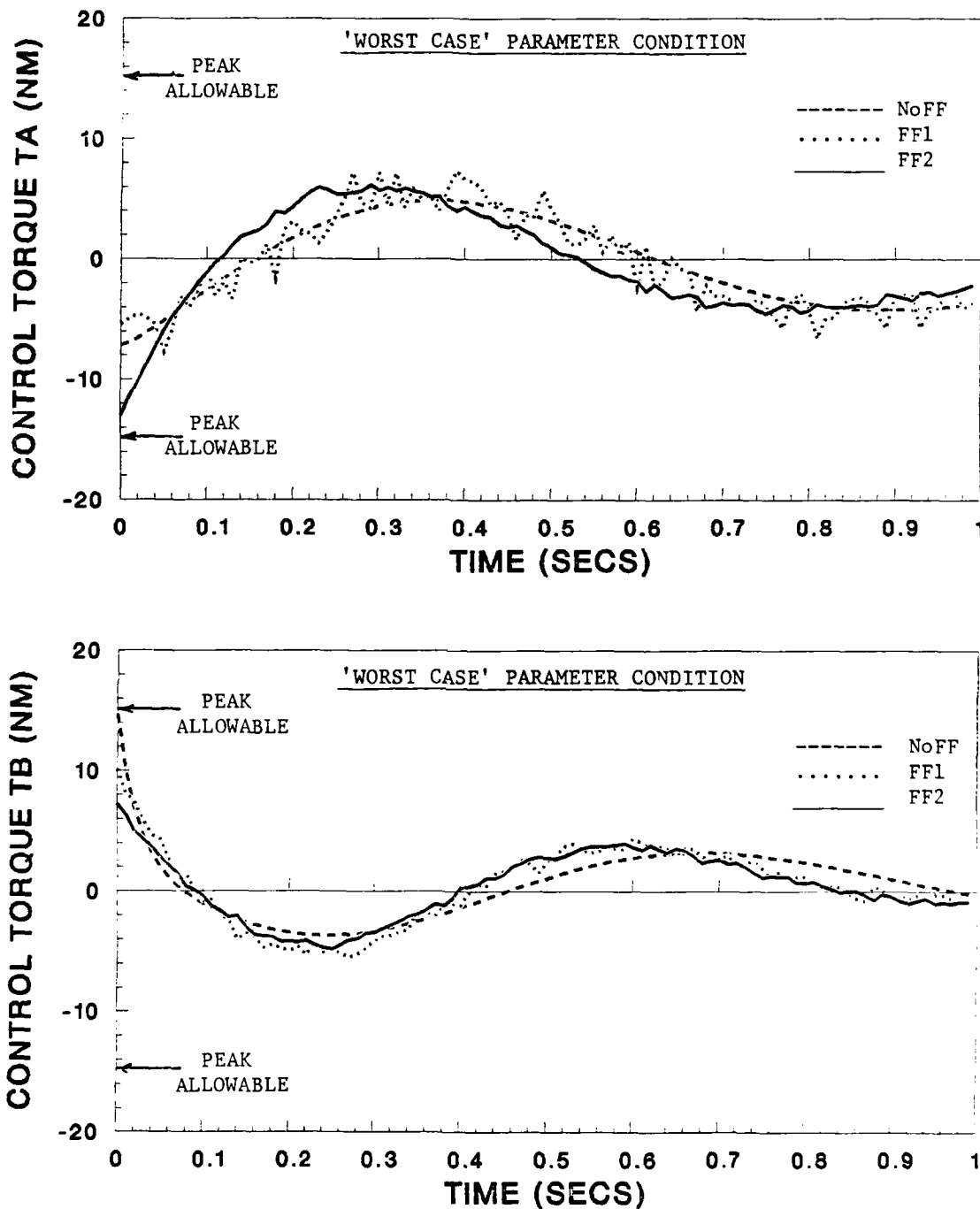


FIG. 20 CONTROL TORQUE HISTORIES OF TRACKING CONTROLLERS WORST PARAMETER CASE
Control torque histories producing tracking error responses of Fig. 19. All three controllers exhibit comparable control effort. Peak and continuous constraints are satisfied in each case

7.0 CONCLUSIONS

This design study has demonstrated that the addition of feedforward compensation to a basic feedback-only (NoFF) controller structure for a target-tracking mechanical arm can provide a marked improvement in the arm's ability to track an oscillating target for a given level of control effort despite variations or uncertainties in the dynamic parameters of both arm and target. In particular, a single-link, single actuator version of the tracking design problem was used to show that, in the absence of feedforward measurement noise, inclusion of either full state feedforward (FSFF) or its near equivalent using target position measurement together with an approximate differentiation network to obtain target rate produced large reductions in average transient and steady-state tracking errors relative to the NoFF structure given the same constraints on control effort. Furthermore, this relative improvement is seen to increase as the target frequency and arm tip mass variability ranges increase (see Figs. 11-12). As noise is introduced into the feedforward measurements, however, it was seen (Figs. 13 and 14) that the use of target position coordinate measurements only (FF1) resulted in a tracking performance which degraded significantly for increasing levels of nearly "white" sensor noise. By contrast, with feedforward using both target position *and* rate coordinated measurements (FF2), a considerable performance improvement was achieved even at fairly high intensities of white noise in all feedforward measurements.

The design comparison conducted for the two-link, two-actuator model of the arm confirmed the trends observed for the single-link, single actuator case at design values for arm tip mass/target frequency variability range factors and feedforward measurement noise intensity. The FF2 controller was shown to provide a (44%) reduction in average root mean square transient tracking error and an (88%) reduction in average root mean square steady-state error relative to the NoFF structure for the same constraints on control effort (Table 5). Furthermore, this structure was the only one to meet all design goals discussed in Section 2.0. It was also determined that a (33%) increase in the peak allowable torque would be required for the FF1 structure to achieve the same

average tracking accuracy as the FF2 structure, while a (167%) increase would be required for the NoFF structure.

This report has attempted to predict, in consistent and quantitative fashion, the improvements attainable by including feedforward in the overall target-tracking control scheme for a mechanical arm. Final decision on the choice of the overall feedforward/feed-back controller structure should weigh the results predicted against the complexities and costs associated with implementation of the structure.

8.0 REFERENCES

1. Greenwood, D., Principles of Dynamics, Prentice-Hall, Englewood, N. J., 1965.
2. Horowitz, I., and Shaked, U., "Superiority of Transfer Function Over State-Variable Methods in Linear Time-Invariant Feedback System Design", *IEEE Trans. on Auto. Cont.*, Vol. AC-20, No. 1, February 1974.
3. Tashker, M., "Integral Control of a Spinning Drag-Free Satellite", Stanford University, SUDAAR 472, April 1974.
4. Gardner, B., "Feedforward/Feedback Control Logic for Robust Target-Tracking", (Ph.D. Thesis to be published as a SUDAAR report, March 1984).
5. Ly, U., "A Design Algorithm for Robust, Low-Order Controllers", Stanford University, SUDAAR 536, November 1982.
6. Bryson, A. E., and Ho, Y., Applied Optimal Control, Hemisphere Publishing Company, Washington, D.C., 1975.

END

FILMED

3-85

DTIC

All three control
tinuous constrain